Submitted to Nuclear Physics

UCRL-19986
Preprint C.2

IN-BEAM GAMMA-RAY SPECTROSCOPY OF EVEN Mo AND Ru ISOTOPES

C. M. Lederer, J. M. Jaklevic,
and J. M. Hollander

November 1970

AEC Contract No. W-7405-eng-48

TWO-WEEK LOAN COPY

This is a Library Circulating Copy which may be borrowed for two weeks. For a personal retention copy, call Tech. Info. Division, Ext. 5545

UCRL-19986 C.2

LAWRENCE RADIATION LABORATORY
UNIVERSITY of CALIFORNIA BERKELEY

DISCLAIMER

This document was prepared as an account of work sponsored by the United States Government. While this document is believed to contain correct information, neither the United States Government nor any agency thereof, nor the Regents of the University of California, nor any of their employees, makes any warranty, express or implied, or assumes any legal responsibility for the accuracy, completeness, or usefulness of any information, apparatus, product, or process disclosed, or represents that its use would not infringe privately owned rights. Reference herein to any specific commercial product, process, or service by its trade name, trademark, manufacturer, or otherwise, does not necessarily constitute or imply its endorsement, recommendation, or favoring by the United States Government or any agency thereof, or the Regents of the University of California. The views and opinions of authors expressed herein do not necessarily state or reflect those of the United States Government or any agency thereof or the Regents of the University of California.

IN-BEAM GAMMA-RAY SPECTROSCOPY OF EVEN Mo AND Ru ISOTOPES†

C. M. Lederer, J. M. Jaklevic, and J. M. Hollander

Lawrence Radiation Laboratory
University of California
Berkeley, California 94720

November 1970

Abstract

Excited states of ^{92,94,96,98}Mo and ^{94,96,98,100,102}Ru were studied by in-beam γ-ray spectroscopy. The decays of levels populated by the (α,2n) reaction on even isotopes of Zr and Mo were studied by measurement of the γ singles spectrum, beam-γ-delay, γγ-coincidences (prompt and delayed), and γ-ray angular distributions. The most notable new feature of these experiments is the use, in-beam, of a sensitive coincidence technique, employing two Ge(Li) spectrometers in conjunction with a two-parameter incremental data-acquisition system, to establish the placement of weak transitions. The level schemes are compared with previous studies of these nuclei. A considerable number of new levels, predominantly of high spin (I > 6), were observed.

The observed levels are analyzed in terms of systematics and, where available, detailed shell-model calculations. A general description in terms of excitations in the low-lying orbitals outside a 38-proton + 50-neutron core appears adequate to explain much of the data, particularly in those nuclei near the 50-neutron shell. The data are also compared to recent macroscopic calculation of quasi-rotational bands, the VMI model.

The observed spin distribution in the residual nuclei indicates a net loss of angular momentum in the emission of neutrons and/or unresolved γ rays.

†Work performed under the auspices of the U. S. Atomic Energy Commission.

Calculations based on a microscopic model for neutron evaporation suggest that, with a moment-of-inertia parameter $\mathfrak{J} = 0.5\ \mathfrak{J}_{rigid}$, the angular-momentum loss can be accounted for entirely by the neutrons, whereas for $\mathfrak{J} > 0.5\ \mathfrak{J}_{rigid}$, some of it must reside in the unplaced γ-ray transitions.

E

NUCLEAR REACTIONS $^{90,92,94,96}Zr$, $^{92,94,96,98,100}Mo(\alpha,2n\gamma)$; measured E_γ, I_γ, $\alpha\gamma(\theta)$, $\alpha\gamma(t)$, γγ-coin. $^{92,94,96,98}Mo$, $^{94,96,98,100,102}Ru$ deduced levels, J, π. $^{92,94}Mo$, ^{94}Ru deduced $t_{1/2}$ (levels). Enriched targets. Ge(Li) detectors.

1. Introduction

Studies of γ rays following (α,xn) reactions on targets of separated, even isotopes of Zr and Mo, conducted during the past three years, have yielded a large body of data on excited states of 16 nuclides. We have already discussed the level schemes of the 50-neutron nuclei ^{92}Mo and ^{94}Ru in a preliminary report[1]). In this paper we describe the experimental methods, present the resultant data, and discuss the levels of the other even isotopes $^{94-98}$Mo and $^{96-102}$Ru. Data on the odd-neutron isotopes and level schemes of ^{95,97}Mo and 93(?), ^{95,97,99,101}Ru are discussed in a separate paper[2]).

2. Experimental Procedures

2.1. TARGETS AND BOMBARDMENTS

Targets of isotopically enriched, even isotopes of Zr and Mo were irradiated with α particles at the Berkeley 88-inch cyclotron to produce excited states of Mo and Ru nuclei via (α,xn) reactions. In most measurements an α-particle energy of 30 MeV, near the peak of the (α,2n) cross-section, was used; in a few the beam energy was 24 or 40 MeV. Most of the targets were in the form of powdered oxide affixed to a 1/4-mil mylar strip with a dilute cement solution. Target thickness, $\approx$ 5-20 mg/cm^2, was sufficient to stop recoiling reaction products, while degrading the beam energy only a few MeV. A few of the observed γ rays were common to most spectra: 110, 197, and 1236 keV (^{19}F)[3]; 184 and 937 keV (^{18}F)[4]; 1887 keV (^{18}Ne)[5]; 275 and 1226 keV (^{19}Ne)[6]. All these can be accounted for by α-particle reactions on ^{16}O in the targets. Metallic foils (of ^{98}Mo and ^{100}Mo) were used in some experiments, with the resultant elimination of these impurity lines. Annihilation quanta, arising both from the build-up of positron emitters (delayed) and from pair production by high-energy gamma rays (prompt) were observed in all targets.

The cyclotron beam-line configuration is shown in fig. 1. The absence of slits in the vicinity of the target and the large shield ahead of the beam stop reduce the background from neutrons and γ rays to a negligible level with an empty target frame in place. Some background, principally from neutrons[7], results from interactions in the target itself.

2.2. γ-RAY ENERGIES, INTENSITIES, AND HALF-LIVES

Spectra were measured with small, planar Ge(Li) detectors ($\approx$ 5 cm^3), placed close to the target at 126° to the incident beam direction in order to reduce

the effect of angular anisotropies ($P_2(\cos 126°) = 0$). Typical resolution was $\approx$ 1.5 keV at 100 keV and $\approx$ 3 keV at 1 MeV. The basic electronic configuration (fig. 2) is a modified version of that described in ref. 7. A conventional high-rate amplifier system[8]) provides an energy signal, while a time signal is produced by a time-to-amplitude converter (TAC) started by the γ-ray pulse and stopped by a (delayed) pulse generated at the upward zero-crossing point on the cyclotron RF voltage. The time signal is further processed in two ways:

1. An "energy-walk" compensator corrects for the energy-dependent time shift introduced by the leading-edge discriminator[9]).
2. Variations in the RF phase relative to the arrival of beam bunches at the target are compensated by a variable-baseline feedback loop, which stabilizes the position of the prompt γ-ray peak in the time spectrum.

The lower limit of detectable half-lives, 2 to 3 ns, is determined primarily by the time resolution of the detector-electronic system. The upper limit is determined by the time interval between beam bunches, $1/\nu_{RF}$, = 163 ns for a 30 MeV α-particle beam. γ rays with lifetimes much longer than this (including transitions which follow beta decay of radioisotopes produced in the target) appear to have an intensity constant in time. In one experiment, we used the microsecond-pulsed beam at the Berkeley HILAC to measure a 77 μs half-life.

The following procedure was adopted for the measurements of γ-ray energies, intensities, and lifetimes: The energies and total intensities for an energy range 0 to 2 MeV (0 to 3 MeV in the case of ^{90}Zr and ^{92}Mo targets) were first measured as a 4096 channel singles spectrum. (Energy and intensity calibrations were done in separate measurements with radioactive standard sources.)

Next, isomeric transitions were sought by measuring 2-dimensional energy vs. time spectra, with 512 channels on the energy axis to cover intervals of ≈ 600 keV and 8 channels to cover the time interval during and between beam bunches. If isomeric transitions were observed, they were further studied in measurements of small energy intervals by employing more channels on the time axis.

The estimated precision of our energy measurements for strong transitions, ≈ 0.1 to 0.2 keV, is consistent with the observed agreement for crossover-cascade relationships. However, the use of external calibrations introduces additional, systematic uncertainties into the absolute energies. We feel that a standard error ±1 keV on all γ rays is a reasonable estimate of the overall uncertainty. Energies measured in our experiments are given on the decay schemes. Where more accurate values are known, they are referred to in the text.

All spectra were analyzed with an on-line shape-fitting program[10]) on a CDC-6600 computer.

2.3. $\gamma\gamma$ COINCIDENCES

A smaller chamber, which permits positioning of both detectors close to the target, was used in most of the $\gamma\gamma$-coincidence measurements. The two detectors were placed at right angles to each other and to the incident beam: a downward-facing 12 cm^3 planar Ge(Li) detector and a horizontal 35 cm^3 coaxial Ge(Li) detector, for which the source-to-target distances were about 1 cm and 3 cm, respectively.

The electronics circuitry is similar to that shown in fig. 2, except that the "stop" signal for the TAC is provided by the second detector, "energy walk" compensation is provided for both detectors, and no time stabilization is needed. When a coincidence occurs within one or two adjustable windows on the

time spectrum, the energy signals from each detector are analyzed in a multiplexed 4096-channel ADC. Normally, one of the time windows is centered on the prompt coincidence peak, and the second is set to record "chance coincidences" between γ rays produced by adjacent beam bursts, events delayed by $\Delta T = 1/\nu_{RF}$. The observed true/chance ratio was ≈ 100. Delayed coincidences can also be recorded by setting one of the time windows slightly off the prompt peak.

Channel numbers corresponding to the energies of each γ ray, and a flag indicating whether the event was a "true" or "chance" coincidence, were stored in the buffer memory of a PDP-5 computer and periodically written onto a magnetic tape. A total of $\approx 10^7$ events were recorded for each target. The tapes were later scanned on the CDC-6600 computer to produce spectra from one detector coincident with a specified transition in the other. These spectra, corrected for chance coincidences and background in the gating detector, were then analyzed in the same manner as the singles spectra. In order to establish quantitative coincidence relations, the coincidence intensities were corrected for detector efficiencies and normalized to the singles intensity of the strongest well-established cascade in each nucleus.

As described below, the coincidence results were in most cases crucial to the assignment of weak transitions to the correct reaction product, as well as to the construction of level schemes. The sensitivity of these measurements therefore sets limits on the placement of weak transitions. Coincidences between two high-energy (≈ 1 MeV) γ rays could in general be ascertained if their coincidence intensity were greater than $\approx 5\%$ of the strongest transition in the spectrum. Better sensitivities were obtained for high-low coincidences (low ≈ 200 keV) or low-low coincidences, about 1% and 0.2% coincidence intensity, respectively.

2.4. ANGULAR DISTRIBUTIONS

Angular distributions relative to the incident beam were measured with the detector configuration shown in fig. 1. Measurements were made with the movable detector at 6 or 7 different angles between 90° and 157° to the incident beam. A second, fixed detector at 45° provided normalization to correct for beam intensity variations. Spectra from the two detectors were recorded simultaneously, and the dead-time in each counting system was monitored by adding the same number of pulser pulses to each spectrum. After analysis of the spectra, the relative intensity of a given transition at each angle was simply computed as

$$W_\gamma(\theta) = \frac{C_\gamma^M}{\sum_\gamma C_\gamma^F} \times \frac{C_{pulser}^F}{C_{pulser}^M} ,$$

where C_γ is the number of counts in a γ-ray peak and the M's and F's refer to the movable and fixed detectors. The sum on C_γ^F is taken over the strongest γ rays from the desired reaction.

The resulting angular distributions were fitted by least squares to the expression

$$W_\gamma(\theta) = \text{const} \times [1 + A_2P_2(\cos\theta) + A_4P_4(\cos\theta)] .$$

The values of A_2, A_4, and the standard deviations are given in Tables 1 to 9.

Because we did not measure intensities at angles greater than 157°, the uncertainties in the small A_4 terms are large. The distributions were also analyzed on the assumption that $A_4 = 0$. Since this did not greatly affect the values derived for A_2 we do not quote these values.

Interpretation of the angular distributions in terms of nuclear structure is considered below. The influence of relaxation effects is also important, especially since our targets were such as to retain poorly the nuclear alignment. A crude measurement of time-differential angular distributions for isomers in ^{92}Mo yields a relaxation lifetime of a few nanoseconds. Since this is about equal to the best time-resolution obtained in these experiments, there may be considerable attenuation of the angular distributions even if a γ ray is not measurably delayed. Although the systematics of these reactions would lead one to believe that, exclusive of a few low-lying isomers, the lifetimes involved should generally be shorter than 10^{-10} s[11]), we cannot be certain that in all cases the observed distributions are not subject to attenuation.

2.5. ASSIGNMENT OF TRANSITIONS AND CONSTRUCTION OF LEVEL SCHEMES

In general, the strongest transitions observed may be assigned to the predominant (α,xn) reaction product expected at a given bombarding energy. Often one or more of these corresponds to a known transition; for instance, the first-excited to ground-state transition in an even nucleus is invariably the strongest one observed, and in most cases its energy is already known. If one of the known transitions follows an isomer, the lifetime of the isomer provides a unique clue to the assignment of other delayed transitions.

In the absence of isomers, most of our isotopic assignments were derived from the coincidence results. In some cases, variation of the bombarding energy or target thickness was used to make assignments. Although variations in the reaction energy do cause changes in the relative intensities of transitions within the <u>same</u> nucleus, due both to energy and angular momentum effects, these are generally found to be smaller than the variations between γ rays assigned

to different reaction products. Experimentally, we have found that assignments based on such excitation considerations almost always agree with those derived from the coincidence results.

When a cascade has been established from a coincidence measurement or the occurrence of several transitions with a common half-life, the ordering of transitions is usually obvious from the relative intensities. If an isomer is present, the isomeric transition is easily distinguished from following transitions by the absence of a prompt component. Cascade-crossover energy relations, so useful for constructing radioactive decay schemes, are of little help in the present experiments. The number of such relationships is small, and the number of γ rays observed in a typical spectrum, on the order of 100, guarantees that a large fraction of these are accidental.

The assignment of spins and parities poses the most difficult problem. These must be inferred from γ-decay patterns and γ-ray angular distributions.

The main difficulty in the interpretation of the angular distributions is that the spins involved are underdetermined by the data. The theoretical description of these distributions[12]) yields possible values of the experimentally determined coefficients A_2 and A_4 in terms of the initial and final spins (I_i, I_f), the multipolarity (and mixing ratio) of the transition, and the alignment of the initial state (α_2, α_4). Even if the alignment and final spin were known, a definite prediction of I_i from the measured A_2 and A_4 would be possible only under the assumption that the transition had a pure multipolarity. In the present case, the alignment is <u>not</u> known. Another difficulty is that α_4 is usually much smaller than α_2[12]), so that the measured A_4's are small and often zero within experimental error.

In spite of these difficulties, angular distributions have proven useful in this type of experiment[7]), because of the fact that the major de-excitation paths seem always to consist of stretched, downward cascades ($I_f = I_i - \ell_\gamma$). Under this restriction, the sign of A_2 is sufficient to determine whether $\ell_\gamma = 1$ or 2 and, consequently, the spin difference $I_f - I_i$. Also, if $\ell_\gamma = 2$ and the transition is not isomeric, it may usually be assumed to be an E2 rather than an M2 transition.

Additional inferences may be made from the fact that alignment is approximately preserved* in a stretched, downward cascade with no side feeding[12,13]). Even in the presence of considerable side feeding, one finds that the transitions in the commonly observed cascade

$$8+ \rightarrow 6+ \rightarrow 4+ \rightarrow 2+ \rightarrow 0+$$

have approximately the same distributions.

We have used extensively considerations of the type discussed above to estimate spins of strongly-populated levels. For weaker transitions, such simple assumptions cannot be expected to hold; in fact, we find that the assumption of stretched, downward transitions frequently leads to self-contradictory sets of spin assignments. In general, the spins of more weakly populated levels are uncertain, but may usually be inferred within one or two units from the de-excitation pattern.

---

*More precisely, all $\ell = 1$ transitions will have the same value of A_2 and all $\ell = 2$ transitions the same values of A_2 and A_4. The alignment (α_2, α_4) is lowered slightly by each transition (see formulas in ref. [12])).

In the following section, γ rays assigned to each even reaction product are summarized in a table. γ rays assigned to neighboring odd-neutron isotopes have been omitted; these are discussed in a separate paper[2]). Deductions concerning the assignment and placement of transitions are given in the last two columns of the tables; the absence of a comment in the last column indicates that the assignment is thought to be certain. Spin assignments are given on the level schemes and discussed in the text; spins in parentheses are probable, while those given in brackets are more speculative values based only on decay patterns and level systematics.

3.1. $^{90}Zr(\alpha,2n)^{92}Mo$ AND $^{92}Mo(\alpha,2n)^{94}Ru$ REACTIONS

A summary of the results for these 50-neutron nuclei has already been published in a preliminary communication[1]). The data are given in Tables 1 and 2 and the level schemes in fig. 3.

It should be noted that the coincidence measurements were of lower sensitivity than those for other reactions studied in this work. We note also that the angular distributions of delayed transitions were measured with a prompt time gate of ≈ 20 ns width. Under this condition, the anisotropies of transitions with strong prompt components (329.7, 773, and 1511 keV in ^{92}Mo; 755 and 1428 keV in ^{94}Ru) are attenuated slightly, while those of the pure 8.8 ns transitions in ^{92}Mo, which have weak prompt components, are strongly attenuated.

The level assignments (fig. 3) have already been discussed in detail[1]). Other information on levels of ^{92}Mo derives from the EC + β^+ decay of ^{92}Tc[14]) and inelastic scattering reactions $(p,p'\gamma)$[15-17]), (α,α')[18]), and (d,d')[19]). The decay of ^{92}Tc (I = 8,9+) populates predominantly the 2762 keV 8+ level. The energies of transitions following the decay of this level are in good agreement with our results. From ^{92}Tc decay the half-life of the 8+ level has been determined as 192 ± 7 ns, and that of the 2614-keV level as 1.50 ± 0.15 ns[14]).

The 5- state and all of the even-parity states that we observed in ^{92}Mo have also been seen in scattering reactions. Numerous additional states have been seen in the (p,p') and (α,α') studies; the only apparent overlap with our results involves a 3- level at 2849 ± 2 keV which decays to the 1511-keV state by a 1340-keV γ ray[17]), possibly identical to the 1338-keV γ ray which we observe but have not placed in the level scheme. An alternative placement for this transition between a level near 4096 keV and the 8+ level is

suggested by the ^{92}Tc decay scheme[14]). With this possible exception, none of the proposed states between 4 and 7 MeV populated weakly in the decay of ^{92}Tc were observed in our experiments. Our data are presently the only results on the excited levels of ^{94}Ru.

3.2. ^{92}Zr (α,2n)^{94}Mo

This is the only even nucleus with N > 50 in which we find an isomer ($t_{1/2} \gtrsim 5$ ns). Its half-life, as derived from a weighted average of the half-lives of the delayed transitions, is (109 ± 10) ns.*

The level scheme is shown in fig. 4. Absence of prompt components in the decay of the 83.6- and 531.9-keV transitions indicates that these proceed directly from the isomeric level. Placement of the transitions of 202.8, 292.8, 305.6, 365.2, 484.5, 598.4, 911.6, 941.3, and 1052.3 keV above the isomeric level is supported by (γ)(delayed-γ)-coincidence measurements. Prompt coincidence spectra lend some support to the placement of the 727.4- and 1166.3-keV transitions. The placement of most other γ rays is well established by coincidence relations, except for the 61.7-, 261.7-, 385.4-, and 1868.9-keV transitions, which are tentatively placed on the basis of energy differences only.

Transitions of 449.2 and 532.1 keV have been observed[21,22]) in the EC + β^+) decay of 5-hour ^{94}Tc (I = 6,7+). Aras et al.[21]) assign the 449-keV transition to the 2870-keV level and have not assigned the 532-keV transition, whereas Barette et al.[22]) place both transitions differently than we do. It seems likely that these two transitions are identical to the 448.7- and 531.9-keV transitions which we observe in the (α,2n) reaction, i.e., that the isomeric level is populated by ^{94}Tc decay. This implies that the placements proposed by Barette et al. are incorrect. It should be noted that the more precise γ-ray energy measurements

*The value reported in ref. [20]) (86 ns) contains a calibration error.

of Barette et al. indicate that our values are systematically low, by about 0.8 keV at 800 keV.

The spin assignment of the isomer may be derived as follows: Spins of the levels at 870 keV (2+), 1572 keV (4+), and 2421 keV (6+) are already well established[23-25,21]). The 531.9-keV transition feeds the 6+ state; its partial lifetime indicates that it is either an M2 (0.06 single particle units[26]), or an E2 (1.7×10^{-3} spu). The spin-parity of the isomer is thus 8- or 8+. The 83.6-keV isomeric transition is a pure E2, according to its conversion coefficient. (Its partial lifetime corresponds to enhancement by a factor of 2 over the single-particle E2 value[26]). The spin of the 2870-keV level is thus 6, with the same parity as the 2953-keV level.

The large retardation that would be implied by the lifetime of the 531.9-keV γ ray if it were an E2 transition seemed so improbable that we had previously made a definite odd-parity assignment to the isomeric level[20]). However, on the basis of theoretical considerations, Ball proposed recently that these levels might have the two-proton configuration $(g_{9/2})^2$ 8+, 6+, while the 2421-keV 6+ state is predominantly a $(d_{5/2})$ $(g_{7/2})$ two-neutron state[27]). In this hypothesis, retardation of the 531.9-keV transition and enhancement of the 83.6-keV transitions are to be explained by the predominant proton or neutron character of the states. The observation of states at 2875 ± 5 and 2960 ± 5 keV populated strongly by the reaction ^{93}Nb(^{3}He,d) with $\ell_p = 4$[28]) supports this hypothesis, if indeed these are identical to our 2870-keV and 2953-keV states. On the other hand, this hypothesis does not explain well the absence of a transition from the 2870-keV state to the 1572-keV 4+ state. The question of the parity of these states remains to be resolved by measurement of the conversion coefficient of the 531.9-keV transition.

The state at 2608-keV is assigned (5-) by analogy with the $(g_{9/2})$ $(p_{1/2})$ proton states observed in the 50-neutron nuclei at about this energy. This assignment is also supported strongly by the observation of the state in the (^{3}He,d) reaction with $\ell_p = 1$[28]. The angular distribution of the 1036-keV γ ray from this state also yields a spin of 5 upon the assumption that it is a "stretched downward" transition. With the same assumption, levels at 3357 and 3364 keV can be assigned tentatively as 8+ and 7- states on the basis of the angular distributions, while the 3894-keV level is assigned a spin of 10 and the same parity as the isomeric state, to which it decays. Rough estimates may be made for other levels on the basis of decay patterns: 3318 keV (I = 8 to 10), 3803 keV (I = 9 to 12), 4005 keV (I = 8 to 10), 4187 keV (I = 11,12), and 4493 keV (I = 10 to 12).

Some other levels of ^{94}Mo have been seen in the (^{3}He,d) reaction[28]. One of these, an even parity level at 2295 ± 5 keV, may be identical to our tentatively assigned level at 2300 keV. A number of low-spin states, observed in the decay of 52 minute ^{94m}Tc (I = (2+) [21,22]) are not appreciably populated by the (α,2n) reaction. In particular, the second 2+ state at 1864 keV is populated with an intensity < 2% of the 870 keV state. A 3- level at ≈ 2.59 MeV, populated in the (d,d') reaction[19], is fed with an intensity $\lesssim$ 3% in our experiments.

Transitions in ^{94}Mo populated by (α,xn) reactions have also been studied at the Research Institute for Physics in Stockholm. A preliminary report of this work[29] includes a scheme of the more strongly populated levels in agreement with fig. 4.

3.3. $^{94}Zr\ (\alpha,2n)\ ^{96}Mo$

The predominant de-excitation path in ^{96}Mo is

$$3787\ (10+) \xrightarrow{(E2)} 2979\ 8+ \xrightarrow{E2} 2441\ 6+ \xrightarrow{E2} 1628\ 4+ \xrightarrow{E2} 778\ 2+ \xrightarrow{E2} gs\ 0+ \quad .$$

From the angular distribution data, the spin-parity assignments are quite certain for all but the weakly populated (10+) state, for which the assignment is quite probable. A second observed branch is

$$3916 \longrightarrow 3370\ (8+') \xrightarrow{(E2)} 2441\ 6+ \longrightarrow \text{etc.} \quad ,$$

where the spin-parity of the second 8+ state is also quite probable (from the angular distribution of the 929.3-keV γ ray). Higher lying, weakly populated states at 4533, 4584, and 4795 keV probably have spins $\geqslant 10$.

A number of lower-lying states which receive moderate-to-weak feeding can best be discussed with reference to existing information on the decay of ^{96}Tc (7+), ^{96m}Tc (4+), and ^{96}Nb (6+)[30-34]. The 1498-keV 2+' state is well established[30,35]; in addition to the 719.9-keV transition to the 2+ state, it decays to the ground state by a transition too weak to be observed in our spectra. Well-established levels at 1869, 1978, 2439, and 2754 keV have been assigned spin-parity 4+, 3+, 5+, and 6+ respectively[30]. Besides the transitions shown in fig. 5, these states also decay by a number of weaker transitions observed only in radioactive decay studies. Their spins seem quite well established* from the beta feedings and decay patterns[30], conversion coefficients[32,33], and

*While there has in the past been some disagreement on the spin-parity assignments[32,33], those reported by Monaro et al.[30] seem quite firm on the basis of all decay data and the present results.

$\gamma\gamma$-angular correlations[30,36-38]). It is interesting to note that, if the spin assignments are correct, our angular distributions indicate that the 2439-keV 5+ state is strongly aligned by the (α,2n) reaction, whereas the 1869-keV 4+' and 2754-keV 6+' states are not. The lowest 4+ and 6+ levels, strongly populated by the (α,2n) reaction, are by contrast quite strongly aligned.

A very probable state at 2219 keV (4+") and a tentative state at 2875 keV (7,8+) have also been reported[30]). The former, populated in the decay of both ^{96}Tc and ^{96}Nb, was not observed in the (α,2n) reaction. The latter, if it exists, decays predominantly to the 2441-keV 6+ state by a 434.8-keV transition. The weak γ ray which we observe at this energy shows weak coincidence relations that would be consistent with this placement. However, a spin-parity of 8+ for the state seems unlikely, since there are at least one and possibly two 8+ states at slightly higher energy. 7+ seems unlikely on grounds of systematics (see discussion in following section).

A striking difference between the (α,2nγ) level scheme for ^{96}Mo and those for ^{92,94}Mo and ^{94,96}Ru is the absence of strongly populated odd-parity states, particularly the regularly occurring 5- state. We have considered the possibility that the 2439-keV level is a 5- rather than a 5+ state. This would be inconsistent with the conversion coefficient of the 569.1-keV transition[32,33]), except in the unlikely event that this transition were an E1 with a large M2 admixture. A further consequence of a 5- assignment to this level would be an odd-parity assignment for the 1978-keV spin-3 level. This is also highly improbable, both because of the conversion coefficient of the 1200.1-keV transition[32,33]), and from the fact that a different 3- state at $\approx$ 2.25 MeV has been identified in the ^{96}Mo(d,d')[19]), and ^{95}Mo(n,γ)[39]) reactions.

The only remaining candidate for the expected 5- state is the 2734-keV level. The angular distribution of the 1105.8-keV transition from this state indicates a possible spin-5 assignment, and we have tentatively assigned it as the 5- state. On this hypothesis, the "probable" level at 3473 keV has a decay pattern consistent with that expected for a 7- state.

Mesko et al. have proposed a level scheme[29]) for ^{96}Mo based on their (α,2nγ) measurements and level schemes derived from radioactive decay studies and recent ^{95}Mo(n,γ) results[40]).

There is general agreement with our level scheme, although Mesko et al. do not report the levels at 3370, 3916, 4533, 4584, and 4795 keV. The only disagreement concerns placement of the 1106-keV γ ray.

A number of additional, weak transitions in the scheme of Mesko et al. were not observed by us. Since these depopulate states of relatively low spin, they may be accounted for by the lower bombarding energies used in some of the Stockholm experiments.

3.4. ^{96}Zr(α,2n)^{98}Mo

The coincidence data were essential for the resolution of some transitions in ^{98}Mo from interfering radiations. With the bombarding energy 30 MeV (and a thick target), the cross-section of the ^{96}Zr(α,3nγ) reaction was found to be 35% of the (α,2nγ) cross-section. A particular problem arises from the fact that transitions of $\approx$ 723 keV and $\approx$ 752 keV were found to occur in both ^{97}Mo and ^{98}Mo. The weaker components of each of these doublets (752.8 keV in ^{98}Mo and 723.1 keV in ^{97}Mo) were detected only in the coincidence spectra. The transition of 510.5 keV, obscured in singles spectra by annihilation radiation, was unambiguously established and placed in the ^{98}Mo level scheme by its coincidence relations. A number of

weak transitions, mostly of low energy, could not be placed unambiguously, although a preponderance of coincidence relations with other transitions in ^{98}Mo provides strong evidence for their assignment to that nucleus (see Table 5, last column).

Of the levels shown in fig. 6, those at 788, 1432, 1510, 2017, and 2679 keV are also populated in the decay of 51 minute ^{98}Nb (I = 4,5+)[41,42]. A level at 2344 keV, reported tentatively[41,42] in the decay of ^{98}Nb, is confirmed by the present results. Other levels of ^{98}Mo found in the decay of 51 minute ^{98}Nb (2224, 2333, 2419, 2767, 3021, 3050, 3211, and 3326 keV) and in the decay of 2.8 second ^{98}Nb (1+)[41,43] (736 keV (0+) and 1761 keV (1,2+) are not detectably populated by the (α,2n) reaction.

The levels at 788, 1432, and 1510 keV have previously been assigned spins and parities 2+, 2+, and 4+ respectively[41,35]. The 2017-keV state is probably the same as the 2.04-MeV 3- state populated strongly by the reaction ^{98}Mo(d,d')[19]. The 2344-keV state is assigned 6+ on the basis of its strong population and the angular distribution of the 834-keV γ ray.

The 2621-keV state is assigned tentatively 5- on the basis of the angular distribution of the 1110-keV γ-ray and the energy systematics of the 5- states in this region. This assignment may be considered certain if the 2017-keV state, to which it also decays, is in fact a 3- state. Definite observation of decay of the 5- state to the 3- state was made in this study only in the case of ^{98}Mo, although there is tentative evidence for this decay pattern also in ^{100}Ru.

The 3272-keV state is assigned 8+ with fairly high confidence from the angular distributions. Comparison with the levels of ^{96}Mo suggests an 8+ assignment for the 2854-keV state also, although the angular distribution of the

510.5-keV γ ray from this state could not be determined because of interference from annihilation radiation. The probable assignment (7-) for the 3096-keV state is supported by the angular distribution of the 475.7-keV γ ray and the existence of a crossover transition to the 6+ state. The 3657-keV state is assigned (9-) with less confidence from the decay pattern. Assignments [9-] to the state at 3769 keV and [10+] to the 4150-keV state are very tentative.

Twenty-nine levels of ^{98}Mo below 4 MeV have been observed in the ^{97}Mo(d,p) reaction[44]). Most of the lowest eight can probably be equated with levels observed in the present studies or from ^{98}Nb decay. Because the resolution of the (d,p) spectra is comparatively low and ℓ_n values were not determined, we feel there is insufficient information on which to base a comparison of higher-lying levels observed in the (α,2nγ) and (d,p) reactions. Further (d,p) results would be useful for elucidation of two-neutron components of states observed in this study.

3.5. ^{94}Mo(α,2n)^{96}Ru

The de-excitation pattern of ^{96}Ru consists of two strong cascades above the 1518-keV 4+ state (see fig. 7):

$$3817\ (10+) \xrightarrow{(E2)} 2950\ 8+ \xrightarrow{E2} 2150\ 6+ \xrightarrow{E2} 1518\ 4+$$

and

$$3951\ (9-) \xrightarrow{(E2)} 3291\ 7(-) \xrightarrow{E2} 2588\ 5(-) \xrightarrow{E1,M1} 1518\ 4+ \quad .$$

The spins are assigned from the angular distributions on the assumption of stretched, downward cascades. Additional support for the assignments is inferred from the near constancy of the anisotropies of the E2 transitions.

Odd parity is inferred for the 2588-keV state from systematics. The only "crossover" connecting the two cascades is the weak 1000.0-keV transition between the (9-) and 8+ levels. The 526.3-keV γ ray which we observe corresponds to the energy difference between the (10+) and 7(-) states, but this placement, which would be inconsistent with the assigned spins, is also interdicted by the coincidence results.

Levels at 4262, 4418, 4598, and 4711 keV are also well established by the observed coincidence relations. Since they feed through the 10+ state with no transitions to lower-spin levels, it seems probable that all have spins $\geqslant 10$. The moderately strong 600.9-keV γ ray has a characteristic "stretched, downward $\ell = 2$" angular distribution, which suggests a 12+ assignment for the 4418-keV state. The same assignment for the 4262-keV state, which is more weakly populated, must be considered very speculative.

Other weakly populated states at 2891 and 3543 keV are fairly well established from the coincidence spectra. Those at 4082, 4534, 4799, and 5096 keV are more tentative. The second 2+ state at 1477 keV is well established.

Only the first excited state of ^{96}Ru, observed in Coulomb excitation, was previously known[45,46]. A recent letter[47] reports two new isomers of ^{96}Rh with half-lives 1.5 ± 0.5 minutes and 9 1/4 minutes. The former emits γ rays of 511 keV ($\gamma^{\pm}$) and 833 keV; the latter emits these and also γ rays of 632 and 686 keV. Comparison with our level scheme lends support to these isotopic assignments, particularly that of the longer-lived isomer.

3.6. ^{96}Mo(α,2n)^{98}Ru

The de-excitation pattern in ^{98}Ru (fig. 8) displays remarkable similarities to that of its isotone, ^{96}Mo. In each of these nuclei the predominant decay

path is through the states

$$(10+) \xrightarrow{(E2)} 8+ \xrightarrow{E2} 6+ \longrightarrow \text{etc.}$$

In each nucleus a second 8+ level receives substantial population. Each has, besides its lowest 4+ and 6+ states, a group of levels of intermediate spin (3 - 6) around 2 MeV that receive moderate feeding. And in each nucleus, the 5- and other odd-parity states are weakly populated and therefore difficult to identify. The occurrence of these phenomena in neighboring isotones suggests that they may somehow be related to neutron excitations. The last two characteristics seem peculiar to, or at least enhanced by, the neutron number N = 54.

The 2+, 4+, and 2+' states of ^{98}Ru are well established from Coulomb excitation [46,48]) and from the decay of ^{98}Tc [49,50]). On the basis of our data, assignments 6+ and 8+ to levels at 2223 and 3127 keV, respectively, are strongly indicated. Assignments (8+) to the 3190-keV state and (10+) to the state at 4001 keV are only probable, and the [9-] assignment for the 3852-keV state is very tentative.

Either of the levels 2546 keV or 2656 keV could be assigned as the 5- state. Energy systematics suggest a slight preference for the lower of the two states (see discussion). From their decay patterns, a spin of 5 or 6 is inferred for both.

States at 1797, 2013, and 2266 keV bear a resemblance to the 1869-keV 4+', 1978-keV 3+, and 2439-keV 5+ states of ^{96}Mo. From the angular distributions of the 253.7- and 469.9-keV transitions, it would appear that the positions of the 4+' and 3+ states are reversed in ^{98}Ru. However, it should be emphasized that the data reported here are insufficient to allow firm assignments to be made to any of the three states.

3.7. $^{98}Mo(\alpha,2n)^{100}Ru$

In spite of the scattering of much of the ^{100}Ru de-excitation intensity among numerous weak γ rays, it has been possible to construct a detailed level scheme (fig. 9) from the coincidence spectra. Levels at 540, 1228, 2078, and 3063 keV are assigned to a sequence 2+, 4+, 6+, 8+ on the basis of angular distributions, decay patterns, and their strong population. (The 2+ and 4+ states, as well as the 1363-keV 2+' state, are well established from Coulomb excitation measurements[46]). Spin-parity assignments to more weakly populated states at 2529 keV (5-), 2954 keV (7-), 3507 keV (9-), and 4087 keV (10+) seem reasonably certain from similar considerations. It is noteworthy that the 2954 keV (7-) state decays predominantly to the 6+ state and only weakly to the 5- state, in contrast to the opposite situation in the lighter Mo and Ru isotopes and the intermediate situation in ^{98}Mo. From the angular distribution of the 624.5-keV γ ray, the 3579-keV state is assigned tentatively as a second 9- state. Other spin assignments are deduced from decay patterns.

Numerous levels of ^{100}Ru are known from the decay of ^{100}Tc (1+) and ^{100}Rh (1-). The most recent summary of these levels and of levels assigned from unpublished $^{99}Ru(n,\gamma)$ data[51]) is given in ref. [52]). There is little overlap with our $(\alpha,2n\gamma)$ results because of the relatively low spins of levels populated by radioactive decay and neutron capture. The first four excited states of ^{100}Ru are seen both in our results and in radioactive decay. These include the 1132-keV 0+ state, also tentatively identified in Coulomb excitation[46]); we infer its population in the $(\alpha,2n)$ reaction from our observation of a weak 591.5-keV γ ray. We also assign tentatively a level at 1882 keV which is seen in both ^{100}Rh decay and neutron capture. In addition to the 1342-keV transition to the 2+ state,

the 1882-keV state decays by transitions to the 4+ and 2+' states that are too weak to have been observed by us. Berzins et al.[52]) assign spin-parity 2+ or 3+ to this level, with the latter spin favored. Observation of the state in the (α,2n) reaction also tends to favor the higher spin.

Comparison of our γ-ray energies with the more precise values of Berzins et al.[52]) indicates that ours are systematically too high--by about 0.6 keV at 540 keV.

3.8. $^{100}Mo(\alpha,2n)^{102}Ru$

The coincidence results for ^{102}Ru were of somewhat lower sensitivity due to experimental problems, but nevertheless were adequate to place unambiguously some weaker γ rays (of energy 235.4, 277.1, 292.1, 333.8, 621.5, 680.7, 727.6, 775.2, and 1264.5 keV) that had not been reported in earlier studies of the $^{100}Mo(\alpha,2n)$ reaction[53,54]). These define new levels at 2372, 2650, 2942, 3387, 3434, and 4056 keV (see fig. 10). According to the coincidence results, the "235.4-keV γ ray" is actually an unresolved doublet. (In particular, the two components of the doublet are in coincidence with each other.) The stronger component is definitely placed between the 2942- and 2706-keV levels, while the weaker one is placed between the 2706 keV level and a probable level at 2471 keV.

The 1047.3 keV γ ray is almost certainly not the same as the (1046.59 ± 0.07)-keV transition observed in the decay of both ^{102}Rh isomers[55]). Our coincidence spectra very probably place this γ ray above the 1108-keV 4+ state, whereas the transition observed in radioactive decay was definitely placed between a state at 1521 keV and the first 2+ state[56]). The 1521-keV state is known also to decay by a 418.5-keV γ ray with 1/3 the intensity of the

1046.6-keV transition[55,56]); the 418-keV γ ray is definitely absent in our spectra. Likewise, the 1789-keV (4+) and 2219-keV 5+ levels populated by the decay of 2.9 year ^{102}Rh (I = 5) also were not observed in our experiments. A limit of $\approx$ 2% may be placed on their feeding via the (30-MeV α,2n) reaction, in marked contrast to the situation in ^{96}Mo and ^{98}Ru, where low-lying states of intermediate spin do receive substantial population. A limit of 1% can be set on feeding of a 0+ state at 944 keV, known from the decay of 206 day ^{102}Rh ($I\pi$ = (1-))[55,56]).

The dominant cascade populated by the (α,2n) reaction,

$$2706\ (?) \xrightarrow{?} 1875\ 6+ \xrightarrow{E2} 1108\ 4+ \xrightarrow{E2} 475\ 2+ \xrightarrow{E2} \text{gs}\ 0+ \quad ,$$

has been well characterized* except for the quantum numbers of the initial state and the multipolarity of the initial transition. This 831.4-keV transition has a very weak angular anisotropy; we find $A_2 = 0.10 \pm 0.04$, while Ewan et al.[54]) report $A_2 = -0.03 \pm 0.02$. (The disagreement in sign may not be significant, since the values are within a few standard deviations combined error, and the beam energies and target conditions differ.) Ewan et al. also report a small, but significant negative polarization for the 831.4-keV γ ray which, together with the weak anisotropy, was interpreted to imply mixed (M1 + E2 or E1 + M2) multipolarity. Thus the spin of the 2706-keV state is very probably 5, 6, or 7. Its strong population and decay pattern favor spin 7. Although the mixed multipolarity and short lifetime ($t_{1/2} \lesssim 5$ ns) of the 831.4-keV transition would argue

*by angular distributions (this work and Ewan et al.[54]), polarization measurements (Ewan et al.), and $\gamma\gamma$ angular correlations measured in the decay of 2.9 year ^{102}Rh[56]).

in favor of even parity, we feel that odd parity is more likely on the basis of systematics. In summary, the 2706-keV state is assigned (7-), where the spin is very probable but the parity is speculative.

The 2372-keV state is tentatively assigned (5-) on the basis of systematics and decay pattern, although the angular distribution of the 1264.5-keV γ ray was not measured. If this assignment is correct, it would lend support to the 7- assignment for the 2706-keV state. The assignments given to the levels at 2650, 2942, and 3387 keV are dependent on the spins and parities of the 2372- and 2706-keV states, and are therefore very tentative.

Transitions of 628.0 and 1104.0 keV can be assigned reliably to the decay of the 1104-keV 2+' state by comparison of their energies and relative intensities with those of similar transitions observed in radioactive decay[55,56]). Comparison of our γ-ray energies with those measured by Gehrke and Helmer[55]) shows that ours are systematically about 0.6 keV too high.

4. Discussion

4.1. SHELL-MODEL INTERPRETATION OF THE OBSERVED LEVELS

In refs. [1]) and [57]) the levels of ^{92}Mo and ^{94}Ru are discussed in terms of the proton configurations $(g_{9/2})^4$, $(p_{1/2})^2(g_{9/2})^2$, and $(p_{1/2})(g_{9/2})^3$. The energies, de-excitation patterns, and all but one of the measured transition probabilities are in excellent agreement with calculations of Ball et al.[57]) based on experimentally determined effective interactions in this two-orbit configuration space. It is remarkable that only one level observed in our study of these nuclei, the 4597-keV (I = 12) level of ^{92}Mo, may fall outside this description. Peker has suggested an interpretation of this level as the $(g_{9/2})^4$ I = 12 state[58]), although the calculations of Ball et al.[57,59]) place such a state higher in energy. Thus, it appears that the levels of ^{92}Mo and ^{94}Ru populated by the (α,2n) reaction can be described by the hypothesis of an inert 50-neutron + 38-proton core[60-63]).

For isotopes with N > 50, numerous additional excitations are possible. The lowest of these are expected to be $(\nu d_{5/2})^2$ I = 2,4 excitations.* Such excitations can also couple to proton excitations to give seniority-4 $(\nu d_{5/2})^2(\pi g_{9/2})^2$ and $(\nu d_{5/2})^2(\pi p_{1/2})(\pi g_{9/2})$ states, as well as states of higher seniority. Other states can arise from the excitation of neutrons to the higher orbitals: $s_{1/2}$, $g_{7/2}$, $d_{3/2}$, and $h_{11/2}$. The single-particle energies of these orbitals relative to the $d_{5/2}$ in molybdenum are 1.6, 1.6, 2.0, and ≈ 2.3 MeV, respectively[64]).

---

*Here and in the discussion below we sometimes omit the configurations of paired particles, i.e. $(g_{9/2})^2$ may represent a seniority two-state of the configuration $(g_{9/2})^n$ or $[(p_{1/2})^2_{0+}(g_{9/2})^{n-2}]$.

The existence of a relatively large energy gap above the $d_{5/2}$ subshell has encouraged several authors[63,65,66]) to calculate levels of ^{94}Mo and ^{96}Mo ignoring higher neutron orbitals. In fig. 11 the calculated[65,66]) levels of ^{94}Mo [configurations $(\nu d_{5/2})^2(\pi p_{1/2})^2(\pi g_{9/2})^2$ for even parity states, $(\nu d_{5/2})^2(\pi p_{1/2})(\pi g_{9/2})^3$ for odd-parity states], and ^{96}Mo [configuration $(\nu d_{5/2})^{-2}(\pi p_{1/2})^2(\pi g_{9/2})^2$] are compared with the experimental levels. We have included only the lowest or lowest few calculated levels of a given spin. Even-parity states of ^{94}Mo including the proton configuration $(g_{9/2})^4$ have also been calculated[66]); these differ very slightly from the levels shown in fig. 11, with the exception of a few additional states arising from $p_{1/2}$ - $g_{9/2}$ pair promotion (eg. the first excited 0+ state is lower by 0.4 MeV). These and odd-parity states of ^{96}Mo have not yet been calculated.

In ^{94}Mo, interpretation of the experimental results is dependent on the uncertain parity of the spin-8 isomeric state (and consequently the parities of the states labelled 6± and 10±, which are connected to the isomer by E2 transitions). If its parity were odd, it would fall outside the quoted theoretical description, since the lowest calculated 8- and 10- states each lie about 1 MeV higher than the observed states. Another interpretation of an 8- (or a 6-) state might be the configuration $(\nu d_{5/2})(\nu h_{11/2})$; from the recent discovery[64]) that the energy of the $h_{11/2}$ single-particle state is rather low (≈ 2.3 MeV) this does not seem unreasonable. A 10- state cannot be formed from these orbitals, but could be ascribed to a seniority-4 excitation $[(\nu d_{5/2})(\nu h_{11/2})]_{8-}(\pi g_{9/2})^2_{2+}$.

On the other hand, if the parities of these states were even, they would be in reasonable agreement with the lowest calculated 6+, 8+, and 10+ states. This interpretation is in agreement with the (^{3}He,d) results[28]), (see subsection

3.2.), in that the lowest calculated 6+ and 8+ states have the predominant configuration[66] $(\pi g_{9/2})^2$. However, the lowest observed 6+ level (2421 keV) is then not explained by the calculations, and must be assumed to involve excitation in other orbitals. In fact, from the low value of log ft for EC decay of ^{94}Tc$[(\nu d_{5/2})(\pi g_{9/2})]_{7+}$ to the 2421-keV 6+ state, Peker has interpreted this state as a $(\nu d_{5/2})(\nu g_{7/2})$ excitation[58], as suggested also by Ball[27].

Other levels of ^{94}Mo show good correspondence with the calculated spectrum. The energy calculated for the second 8+ state is close to that of the 3357-keV (8+) state. The indicated correspondence (fig. 11) between the lowest calculated 12+ and 11+ states and two observed levels of high spin is suggested by their decay patterns, but only if the parity of the "10± state" is in fact even; this hypothesis is at any rate only speculative. The observed 5- and 4- states are known from the (^{3}He,d) study[28] to be predominantly $(\pi p_{1/2})(\pi g_{9/2})$ excitations, as are the calculated states. Thus the observed 5- and 4- states are analogous to the odd-parity, seniority-two excitations in the 50-neutron nuclei[57,67]. The lower-lying 4- state in the calculated spectrum has the dominant configuration $(\pi p_{1/2})(\pi g_{9/2})^3_{7/2+}$, which would not be populated by a single-particle transfer reaction[28]. The (7-) observed state has about the same energy as the lowest calculated 7- state. The calculated wave function[66] has the dominant components $[(\pi p_{1/2})(\pi g_{9/2})]_{5-}$ $(\nu d_{5/2})^2_{2+}$ and $(\pi p_{1/2})(\pi g_{9/2})$ in approximately equal amounts, the latter being the configuration of the 7- states in the 50-neutron nuclei. Either component should decay to the 5- state, in agreement with the observed decay mode. The 3- state, which lies considerably below the lowest calculated 3- state, is thought to be more collective[19].

The even-parity levels of ^{96}Mo also correspond well with the calculated spectrum. Exceptions are the observed 4+', 3+, and 6+ states, which occur well below the calculated energies. The same arguments applied to the lowest 6+ state of ^{94}Mo would favor a $(\nu d_{5/2})(\nu g_{7/2})$ configuration for the lowest 6+ state in ^{96}Mo also[58]). This configuration might also account for the 4+' and 3+ states, although $(\nu d_{5/2})(\nu s_{1/2})$ is an alternative possibility for the 3+ state. Either configuration could account for the high E2 content[30]) of the 3+ → 2+ transition.

In the absence of such detailed calculations of levels in other Mo and Ru nuclei, we attempt here only a more qualitative discussion of the systematics. Figures 12a and 12b illustrate these systematics. The levels shown are those (from previous studies and the present experiments) for which probable spins and parities have been assigned.

A number of smooth trends are evident. The 5- state occurs at very nearly the same energy in most of the nuclei. (It may be a little lower in ^{102}Ru. Its position is not well established in ^{98}Ru; the lower of the two states assigned (5,6) in ^{98}Ru would better fit the 5- level systematics.) This suggests that its structure is predominantly the same as in ^{92,94}Mo and ^{94}Ru: $(\pi p_{1/2})(\pi g_{9/2})$. The 7- and 9- states show a systematic trend with increasing neutron number toward lower energy and a preference for decay to even-parity states (6+ and 8+, respectively). This indicates some change in their structure as neutrons are added. The change in the calculated structure of the 7- state from ^{92}Mo $\{(\pi p_{1/2})(\pi g_{9/2})^3\}$ to ^{94}Mo {the same configuration mixed with $[(\pi p_{1/2})(\pi g_{9/2})]_{5-}(\nu d_{5/2})^2_{2+}$} has already been noted; a similar change {admixture of the configurations $[(\pi p_{1/2})(\pi g_{9/2})]_{5-}(\nu d_{5/2})^2_{4+}$ and $[(\pi p_{1/2})(\pi g_{9/2})^3]_{7-}(\nu d_{5/2})^2_{2+}]$} occurs in the calculated 9- states. Other changes, possibly the addition of such

configurations as $(\nu h_{11/2})(\nu d_{5/2})$, $(\nu h_{11/2})(\nu g_{7/2})$, and $[(\pi p_{1/2})(\pi g_{9/2})^{1,3}]_{5-,7-}(X)^2_{2+,4+}$ ($X = \nu g_{7/2}$, $\nu d_{3/2}$, or $\nu h_{11/2}$) may account for the continued lowering of these levels as even more neutrons are added. (Various combinations of these components may account for the probable second 7- and 9- states in ^{100}Ru.) However, the preference for decay by E1 transitions in the heavier isotopes cannot be explained by any such admixtures; these transitions must be ascribed to (small) admixtures of components involving orbitals in other major shells. Their occurrence in heavier isotopes may be due to increased hindrance of the E2 transitions resulting from changes in the major components of the wave functions.

The energies of the lowest 2+ and 4+ states in Mo isotopes decrease between N = 50 and N = 52 and then remain relatively constant. This has been interpreted[62,63,65] as a change from a nearly pure $(\pi g_{9/2})^2$ configuration to one which is predominantly $(\nu d_{5/2})^2$. The expected filling of the $\nu d_{5/2}$ shell in ^{98}Mo is only partially achieved[63,68]. Although the behavior is similar in Ru isotopes, there is a marked trend toward greater collectivity, as evidenced by continuously decreasing energy and increasing B(E2) values[48].

The lowest 6+ states are probably predominantly $(\nu d_{5/2})(\nu g_{7/2})$ excitations as was already inferred in the discussion of ^{94,96}Mo; their energies are relatively constant. The 8+ and 10+ states show an <u>increase</u> in energy with increasing N, whereas the 8+' state appears to be relatively constant in energy. The calculated structures[66] of these states in ^{94}Mo have the dominant components:

8+ : $(\pi g_{9/2})^2$

10+ : $(\pi g_{9/2})^2_{8+}(\nu d_{5/2})^2_{2+}$

8+' : $(\pi g_{9/2})^2_{6+}(\nu d_{5/2})^2_{2+}$ with smaller contributions from $(\pi g_{9/2})^2_{4+}(\nu d_{5/2})^2_{4+}$ and $(\pi g_{9/2})^2_{6+}(\nu d_{5/2})^2_{4+}$

Similar structures might be expected in the other isotopes, with possible additional contributions from components involving other neutron orbitals in the more neutron-rich isotopes. The reason for the increasing energies of the 8+ and 10+ states is not clear, but may involve either small equilibrium deformations in these high-spin states, which would raise the energy of the high-K substates derived from the $\pi g_{9/2}$ orbital, or increased correlations in the ground states, which would lower their energies relative to the states under consideration.

Even within the limited, 3-orbital ($\pi p_{1/2}$, $\pi g_{9/2}$, $\nu d_{5/2}$) configuration space of the ^{94}Mo calculations, the largest single components of the wavefunctions comprise only ≈ 50% to 80% of the states[66]). For this reason, the simple shell-model configurations calculated or hypothesized in the above discussion can only be considered a partial characterization of the states. The calculations do suggest that certain configurations <u>are not</u> important components[66]). Most notable among these are $(\pi g_{9/2})^4$ excitations of seniority-4, which lie higher in energy than other excitations of the same spin [eg. $(\pi g_{9/2})^2(\nu d_{5/2})^2$], and are probably not important components of the observed states.

4.2. COMPARISON WITH THE VMI MODEL

Mariscotti, Scharff-Goldhaber, and Buck have proposed a two-parameter description of quasi-rotational bands, the "variable moment of inertia model"[69]). In this model, the ratio of energies of the 6+, 8+, 10+ ... states to that of the 2+ state, E_I/E_2, can be predicted as a function of E_4/E_2. The original region of validity, $2.231 \leq E_4/E_2 \leq 3.333$, is extended by the admission of negative values for the moment of inertia parameter, $\mathfrak{J}_0$, to values of E_4/E_2 as

low as 1.826[70,71]). The region $1.826 \leqslant E_4/E_2 \leqslant 2.231$ is referred to as the "spherical" region, since $\mathfrak{J}(I = 0) = 0$, whereas in the "deformed" region $(2.231 \leqslant E_4/E_2 \leqslant 3.333)\ \mathfrak{J}(I = 0) = \mathfrak{J}_0$. Mariscotti[70]) has recently proposed an interpretation of the mathematically equivalent "Harris model" equations[72]) which is valid in the range $1 \leqslant E_4/E_2 \leqslant 1.826$ (the "magic" region[71])). Solutions of the VMI or Harris equations for E_I/E_2 are continuous in the spherical and deformed regions, whereas there is a discontinuity at the boundary of the "magic" region[70]).

Our results are compared with VMI calculations in fig. 14. They include for the first time 10+ states of nuclei in this region. The calculated curves for $E_4/E_2 < 1.826$ (dashed curves) follow the prescription given by Mariscotti[70]). We note that:

1) The trends are in general agreement with the calculated curves.
2) Experimental points for ^{96}Mo fall well below the curves. (Somewhat better agreement would have been obtained if the average energy of the two low-lying 4+ states had been used instead of the energy of the lower one.)
3) ^{94}Mo and ^{96}Ru, which lie slightly inside the "magic" region, do not follow the predicted discontinuity.
4) Although the lowest 10+ states of ^{92}Mo and ^{94}Ru have not been observed, the shell model predictions[57]) for these states lie far above the calculated curve. If in fact the lowest 10+ state lies near the shell-model prediction, a quasi-rotational description of these "magic" nuclei would be superfluous, since the shell model also predicts (even more accurately than VMI) the energies of the other states.

4.3. MECHANISM OF THE (α,2n) REACTION

Although the purpose of these studies was to obtain information about the structure of low-lying states, some data on the distribution of angular momentum in the reaction was also obtained. The (α,2n) reaction process is thought to consist of several distinct steps:

1) Compound nucleus formation, which can be understood in terms of an optical model.
2) Neutron evaporation, whose rate is dependent on neutron-transmission coefficients (functions of $E_{neutron}$ and ΔJ) and the level densities of the initial and final nuclei (functions of E and J). The details of angular momentum transfer in the neutron-emission process are not well understood[73]); in particular, there has been no experimental verification of statistical model, spin-dependent level densities for high-spin states. In some cases γ-ray emission may compete with neutron emission[74]).
3) Gamma ray cascades. For resolved transitions that have been placed in the level scheme, the spins of the initial states in these cascades are known or inferred approximately from the scheme itself.

To illustrate the spin-distributions at various steps of the reaction, we choose the system ^{98}Mo + 28-MeV α (28 MeV is the average lab energy in our thick target); in this case the relatively high sensitivity of the coincidence data permits placement of weaker γ rays in the level scheme. The histogram in fig. 15 shows the experimental spin-distribution in ^{100}Ru (in steps of 2ħ) just before the emission of those γ-rays whose placement is known ("unaccounted feeding" in fig. 9). The solid curve for ^{98}Mo + 28-MeV α, calculated from the optical-model

equations of Huizenga and Igo[75]), is skewed to higher angular momentum, which indicates there is a net loss of angular momentum in decay from ^{102}Ru to the observed states of ^{100}Ru. The two broken curves show the calculated spin-distribution in ^{100}Ru after the emission of two neutrons. These curves were calculated* from the equations of Thomas[76]). The curves for $\mathfrak{J} = \mathfrak{J}_{rigid}$ and $\mathfrak{J} = 0.3\mathfrak{J}_{rigid}$ bracket the experimental results; the value $\mathfrak{J} \approx 0.5\ \mathfrak{J}_{rigid}$ results in a curve which is close to the experimental distribution. ($\mathfrak{J}$, the "moment of inertia", enters as a parameter in the theoretical level densities.)

---

*The probability of neutron emission from a state (E_i, J_i) to a state (E_f, J_f) is given by the equation

$$P(E_i,J_i,E_f,J_f) = \frac{1}{h}\frac{\Omega(E_f,J_f)}{\Omega(E_i,J_i)} \sum_{S=|J_f-\frac{1}{2}|}^{J_f+\frac{1}{2}} \sum_{\ell=|J_i-S|}^{J_i+S} T_\ell(E_{neutron}) ,$$

where Ω is the level density, as given by Thomas[76]), and T_ℓ is the transmission coefficient for a neutron with orbital angular momentum ℓ, as given by Blatt and Weisskopf[77]).

The broken curves in fig. 14 were calculated by integration over the two neutron energies and summation over all intermediate spins. In order to account for those decays which result in the (α,n) or (α,3n) product (whose spin-distributions are different from that of the (α,2n) product), it was assumed that neutron emission will always occur when $E_{neutron}$ for the transition from a state of spin J to an Yrast state of the same spin ($E = J(J+1)\mathfrak{J}$) is positive, and not otherwise. All parameters in these calculations are the same as those which Thomas used for his single-neutron calculations[76]).

We have not taken surface interactions or charged-particle emission into account. Since the (α,p) and (α,pn) cross-sections are found to be relatively small in our experiments, these effects must be small.

If in fact the weak (but possibly numerous), unplaced γ transitions do not carry off significant angular momentum, it may be concluded that the theoretical description (with $\mathcal{J} \approx 0.5\,\mathcal{J}_{rigid}$) provides a satisfactory accounting of angular-momentum loss during neutron emission. The same calculations also predict approximately correct ratios of the gross cross-sections $(\alpha,n)/(\alpha,2n)/(\alpha,3n)$. However, the calculated energy distribution in ^{100}Ru after neutron evaporation is much higher than observed, the predicted average excitation energy being only a few MeV below the neutron separation energy. This would imply that there are numerous, unresolved γ rays of high energy which, however, carry off little net spin.

Acknowledgments

We greatfully acknowledge the help of the staff of the 88-inch cyclotron for assistance in performing the experiments. We are especially indebted to Dr. James Ball for many helpful discussions of the results and for communicating the results of his shell-model calculations which proved so useful for interpretation of the level schemes.

REFERENCES

1) J. M. Jaklevic, C. M. Lederer, and J. M. Hollander, Phys. Letters 29B (1969) 179

2) C. M. Lederer, J. M. Jaklevic, and J. M. Hollander, submitted to Nuclear Physics (1971)

3) A. R. Poletti, J. A. Becker, and R. E. McDonald, Phys. Rev. 182 (1969) 1054

4) M. J. Throop, Phys. Rev. 179 (1969) 1011

5) B. C. Robertson, R. A. I. Bell, J. L'Ecuyer, R. D. Gill, and H. J. Rose, Nucl. Phys. A126 (1969) 431

6) J. W. Olness, A. R. Poletti, and E. K. Warburton, Phys. Rev. 161 (1967) 1131

7) T. Yamazaki and G. T. Ewan. Nucl. Phys. A134 (1969) 81

8) F. S. Goulding, D. A. Landis, R. H. Pehl, University of California Lawrence Radiation Laboratory Report UCRL-17560 (1967) unpublished

9) J. M. Jaklevic, F. M. Bernthal, J. O. Radeloff, and D. A. Landis, Nucl. Instr. Methods 69 (1969) 109

10) C. M. Lederer, in Radioactivity in Nuclear Spectroscopy, ed. J. H. Hamilton, Gordon and Breach Publishing Co., New York (1970), p.

11) R. M. Diamond, F. S. Stephens, W. H. Kelly, and D. Ward, Phys. Rev. Letters 22 (1969) 546

12) T. Yamazaki, Nucl. Data A3 (1967) 1

13) L. C. Biedenharn, Angular Correlations in Nuclear Spectroscopy, ed. by F. Ajzenberg-Selove, (American Press, New York, 1960) Chapter V

14) J. Konijn et al., Inst. for Nucl. Phys. Research, Amsterdam, 1967-68 Progress Report, p. 24

15) J. K. Dickens, E. Eichler, R. J. Silva, and I. R. Williams, Phys. Letters 21 (1966) 657

16) K. P. Lieb, T. Hausmann, J. J. Kent, and C. F. Moore, Z. Physik 217 (1968) 213

17) K. P. Lieb, T. Hausmann, and J. J. Kent, Phys. Rev. 182 (1969) 1341

18) E. J. Martens and A. M. Bernstein, Nucl. Phys. A117 (1968) 241

19) Y. S. Kim and B. L. Cohen, Phys. Rev. 142 (1966) 788

20) J. M. Jaklevic, C. M. Lederer, and J. M. Hollander, Lawrence Radiation Laboratory Chemistry Division Annual Report, 1969, UCRL-19530, p. 49 (1970)

21) N. K. Aras, E. Eichler, and G. G. Chilosi, Nucl. Phys. A112 (1968) 609

22) J. Barrette, A. Boutard, and S. Monaro, Can. J. Phys. 47 (1969) 995

23) L. I. Yin, R. E. Sund, R. G. Arns, and M. L. Widenbeck, Nucl. Phys. 34 (1962) 588

24) C. W. Reich, R. P. Schuman, and R. L. Heath, Phys. Rev. 129 (1963) 829

25) J. H. Hamilton, K. E. G. Löbner, A. R. Sattler, and R. van Lieshout, Physica 30 (1964) 1802

26) S. A. Moszowski, in Alpha-, Beta-, and Gamma-Ray Spectroscopy, ed. by Kai Siegbahn, (North Holland Publishing Co., Amsterdam, 1965), Chapter XV

27) J. B. Ball, private communication (1970)

28) M. R. Cates, J. B. Ball, and E. Newman, Phys. Rev. 187 (1969) 1682

29) L. Mesko, M. Brenner, A. Nilsson, and S. A. Hjorth, Annual Report, Research Institute for Physics, Stockholm, 1969, p. 39

30) S. Monaro, J. Barrette, and A. Boutard, Can. J. Phys. 46 (1968) 2375

31) R. Cesareo, L. Frevert, and A. Flammersfeld, Z. Phys. 205 (1967) 174

32) S. Antman, H. Pettersson, and Y. G. Grunditz, Nucl. Phys. A110 (1968) 289

33) V. A. Ageev, J. Vrzal, J. Liptak, V. K. Maidanyuk, J. Urbanets, and A. I. Feoktistov, Izv. Akad. Nauk SSSR, Ser. Fiz. 32 (1968) 220 (English transl. 32 (1969) 199)

34) V. A. Ageev, V. I. Gavrilyuk, V. I. Kupryashkin, G. D. Latyshev, I. N. Lyutyi, V. K. Maidanyuk, Yu. V. Makovetskii, and A. I. Feoktistov, Izv. Akad. Nauk SSSR, Ser. Fiz. 33 (1969) 1275 (English transl. 33 (1970) 1180)

35) Yu. P. Gangrskii and I. Kh. Lemberg, Izv. Akad. Nauk SSSR, Ser. Fiz. 26 (1962) 1001 (English transl. 26 (1963) 1009); ZhETF 42 (1962) 1027 (English transl. Soviet Phys. JETP 15 (1962) 711)

36) P. Born, N. H. Elsenaar, A. Veefkind, and J. Blok, Physica 29 (1963) 905

37) L. Simons, R. E. Holland, G. Wendt, E. Spring, L. Käld, and E. Hagebø, Nucl. Phys. 39 (1962) 130

38) P. Born, A. Veefkind, W. H. Elsenaar, and J. Blok, Physica 29 (1963) 535

39) J. Eichler, Z. Phys. 219 (1969) 114

40) D. Heck, N. Ahmed, U. Fanger, W. Michaelis, H. Ottmar, and H. Schmidt, Nucl. Phys. A159 (1970) 49

41) K. Hübenthal, E. Monnand, and A. Moussa, Nucl. Phys. A128 (1969) 577

42) P. Koldewijn, Institute for Nuclear Physics Research Progress Report, Amsterdam, 1968-1969, p. 36

43) K. Hübenthal, J. Berthier, J.-C. Hocquenghem, and A. Moussa, Compt. Rend. 265 (1967) 162B

44) K. R. Evans, F. Ajzenberg-Selove, and Baruch Rosner, Phys. Rev. 165 (1968) 1327

45) R. L. Robinson, P. H. Stelson, F. K. McGowan, J. L. C. Ford, Jr., and W. T. Milner, Nucl. Phys. 74 (1965) 281

46) F. K. McGowan, R. L. Robinson, P. H. Stelson, and W. T. Milner, Nucl. Phys. A113 (1968) 529

47) A. H. W. Aten, Jr. and Johanna C. Kapteyn, Physica 33 (1967) 705

48) P. H. Stelson and F. K. McGowan, Phys. Rev. 121 (1961) 209

49) S. Katcoff, Phys. Rev. 99 (1955) 1618

50) S. Katcoff, Phys. Rev. 111 (1958) 575

51) N. C. Rasmussen, V. J. Orphan, Y. Hukai, and T. Inouye, quoted by G. A. Bartholomew et al., Nucl. Data A3 (1967) 609

52) G. Berzins, M. E. Bunker, and J. W. Starner, Phys. Rev. 187 (1969) 1618

53) J. M. Jaklevic, C. M. Lederer, and J. M. Hollander, Lawrence Radiation Laboratory Report UCRL-18667 (1969), p. 15

54) G. T. Ewan, G. I. Andersson, G. A. Bartholomew, and A. E. Litherland, Phys. Letters 29B (1969) 352

55) R. J. Gehrke and R. G. Helmer, Phys. Rev. 177 (1969) 1792

56) J. Konijn, E. W. A. Lingeman, F. Diederix, B. J. Meijer, P. Koldewijn, and A. A. C. Klaasse, Nucl. Phys. A138 (1969) 514

57) J. B. Ball, J. B. McGrory, R. L. Auble, and K. H. Bhatt, Phys. Letters 29B (1969) 182

58) L. K. Peker, Proceedings of the Winter School for Nuclear Theory and High Energy Physics, Physical-Technical Institute, Leningrad, part I (1969) p. 163; University of California Lawrence Radiation Laboratory Report UCRL-Trans.-1399

59) J. B. Ball, private communication (1969)

60) I. Talmi and I. Unna, Nucl. Phys. 19 (1960) 225

61) S. Cohen, R. A. Lawson, M. H. Macfarlane, and M. Soga, Phys. Letters 10 (1964) 195

62) N. Auerbach and I. Talmi, Nucl. Phys. 64 (1965) 458

63) J. Vervier, Nucl. Phys. 75 (1966) 17

64) J. B. Moorhead and R. A. Moyer, Phys. Rev. 184 (1969) 1205

65) K. H. Bhatt and J. B. Ball, Nucl. Phys. 63 (1965) 286

66) J. B. Ball, private communication (1970)

67) R. B. Day, A. G. Blair, and D. D. Armstrong, Phys. Letters 9 (1964) 327

68) Sven A. Hjorth and Bernard L. Cohen, Phys. Rev. 135 (1964) B920

69) M. A. J. Mariscotti, G. Scharff-Goldhaber, and B. Buck, Phys. Rev. 178 (1969) 1864

70) M. A. J. Mariscotti, Phys. Rev. Letters 24 (1970) 1242

71) Gertrude Scharff-Goldhaber and Alfred S. Goldhaber, Phys. Rev. Letters 24 (1970) 1349

72) S. M. Harris, Phys. Rev. 138 (1965) B509

73) J. O. Newton, F. S. Stephens, R. M. Diamond, K. Kotajima, and E. Matthias, Nucl. Phys. A95 (1967) 357

74) J. R. Grover, Phys. Rev. 123 (1961) 267; 127 (1962) 2142

75) J. R. Huizenga and G. Igo, Nucl. Phys. 29 (1962) 462

76) T. Darrah Thomas, Nucl. Phys. 53 (1964) 558, 577

77) John M. Blatt and Victor F. Weisskopf, Theoretical Nuclear Physics, John Wiley and Sons, New York (1952)

Table 1. γ rays from the reaction $^{90}Zr(\alpha,2n\gamma)^{92}Mo$

E_γ, keV[a]	I_γ Relative[b]	Half-life, ns	Angular Distribution[c] A_2	A_4	Placement	Comment
86 ± 2	4.7 ± 1.5	long[d,e]			2614 6+ → 2528 5(-)	
110 ± 2	6.7 ± 2.0	prompt	-0.10 ± 0.04	0.13 ± 0.09	4597(12)→ 4487 (11-)	
148.0	33 ± 3	219 ± 22	-0.05 ± 0.03	0.03 ± 0.04	2762 8+ → 2614 6+	e/γ=0.24 ± 0.10[f]
234.9	22 ± 2	8.7 ± 0.2	0.13 ± 0.04	-0.01 ± 0.07	4487(11-) → 4252(9-)	
244.1	50 ± 10[g]	8.4 ± 0.4[e] ≈ 190	-0.15 ± 0.04	0.00 ± 0.06	2528 5(-) → 2284 4+	
329.7	40 ± 2	240 ± 50[e]	0.14 ± 0.03	0.05 ± 0.05	2614 6+ → 2284 4+	
481?	3 ± 1	prompt				assignm. uncertain
538?	5 ± 2	prompt				assignm. uncertain
626	25 ± 2	9.5 ± 0.5[e]	0.17 ± 0.03	0.00 ± 0.05	4252(9-) → 3627(7-)	
664?	3 ± 1	prompt				assignm. uncertain
740	3 ± 1					assignm. uncertain
773	96 ± 3	8.0 ± 0.7[e] 400 ± 300	0.15 ± 0.03	-0.02 ± 0.04	2284 4+ → 1511 2+	
1097	28 ± 1	10.0 ± 0.9[e]	0.19 ± 0.05	-0.01 ± 0.09	3627(7-) → 2528 5(-)	
1338?	7.0 ± 0.5	prompt				assignm. uncertain
1511	100	9.0 ± 0.9[e] long[d]	0.15 ± 0.04	0.02 ± 0.07	1511 2+ → gs 0+	

(continued)

Table 1. (Continued)

[a] ±1 keV unless otherwise noted.

[b] Total prompt and delayed intensity.

[c] See text for comment on attenuation.

[d] Statistics too poor to determine half-life. Assigned to 220 ± 30 ns component.

[e] Plus a prompt component.

[f] Determined from the relative cascade intensities in the delayed spectrum.

[g] The large uncertainty is due to difficulties in resolving the 244-keV γ from other lines in the prompt spectrum.

Table 2. γ rays from the reaction $^{92}Mo(\alpha,2n\gamma)^{94}Ru$

E_γ, keV[a]	I_γ Relative[b]	Half-life, ns	Angular Distributions[c] A_2	A_4	Placement	Comment
126 ± 2	7 ± 2	prompt	-0.09 ± 0.06	0.02 ± 0.05	2622(5-) → 2495 6+	
145	40 ± 5	73 ± 5 μs[d]	-0.05 ± 0.04	-0.01 ± 0.07	2640 8+ → 2495 6+	
311	61 ± 3	69 ± 5 μs[d] 74 ± 7 ns[e]	0.10 ± 0.05	0.00 ± 0.07	2495 6+ → 2183 4+	
439	16 ± 2	prompt	-0.13 ± 0.06	0.09 ± 0.09	2622(5-) → 2183 4+	
691	≈ 12	prompt	0.29 ± 0.10	0.04 ± 0.15	4346(9-) → 3655(7-)	partially masked in singles spectrum
755	81 ± 3	long[f]	0.21 ± 0.04	-0.01 ± 0.06	2183 4+ → 1428 2+	
1033 ± 2	15 ± 1	prompt	0.34 ± 0.07	-0.25 ± 0.10	3655(7-) → 2622(5-)	
1428 ± 2	100	long[f]	0.25 ± 0.09	-0.11 ± 0.04	1428 2+ → gs 0+	

[a] Energies to ±1 keV unless otherwise noted.

[b] Total of prompt and delayed intensity.

[c] See text for note on attenuation.

[d] Measured with a pulsed α beam at the HILAC.

[e] From a coincidence measurement of the time delay between the 145- and 311-keV transitions.

[f] The 755- and 1428-keV transitions have prompt components plus a complex decay identical to that of the 311-keV transition.

Table 3. γ-rays from the reaction $^{92}Zr(\alpha,2n\gamma)$

E_γ, keV ±1.0	I_γ Relative[a]	$t_{1/2}$, ns	Angular Distributions[b] A_2	A_4	Placement	Comment
61.7?	≈ 0.02				(3865 → 3803)	possibly ^{94}Mo energy diff.
83.6	3.2 ± 0.5	101 ± 18	0.09 ± 0.10	0.06 ± 0.15	2953 8± → 2870 6±	e/γ 2.2±0.3[d]
202.8	0.5 ± 0.2	prompt[c]	-0.18 ± 0.06	-0.06 ± 0.09	4005 → 3803	very probably ^{94}Mo del.coinc.
261.7	0.5 ± 0.2				(2870 6± → 2608(5-))	probably ^{94}Mo, energy diff.
275.0	1.6 ± 0.2	prompt				assignm. uncertain
292.8	13 ± 1	prompt[c]	0.23 ± 0.04	0.01 ± 0.07	4187 → 3894(10±)	
305.6	2.4 ± 0.2	prompt[c]	-0.24 ± 0.04	-0.18 ± 0.16	4493 → 4187	
365.2	4.8 ± 0.3	prompt[c]	0.37 ± 0.04	-0.07 ± 0.06	3318 → 2953 8±	
385.4	0.6 ± 0.2				4187 → 3803	possibly ^{94}Mo energy diff.
448.7	13 ± 1	112 ± 17[e]	0.03 ± 0.07	0.12 ± 0.10	2870 6± → 2421 6+	
484.5	3.7 ± 0.4	prompt[c]	-0.41 ± 0.05	-0.10 ± 0.08	3803 → 3318	
531.9	35 ± 2	108 ± 7	0.00 ± 0.06	0.10 ± 0.09	2953 8± → 2421 6+	
560.5?	1.4 ± 0.4	prompt				possibly ^{94}Mo excit.
569.2	2.0 ± 0.4	prompt				assignm. uncertain
598.4	1.7 ± 0.4	prompt[c]			4493 → 3894(10±)	
651.8	3.7 ± 0.5	prompt	0.19 ± 0.13	0.14 ± 0.20		probably ^{94}Mo, excit.

(continued)

Table 3. (Continued)

E_γ, keV ±1.0	I_γ Relative[a]	$t_{1/2}$, ns	Angular Distributions[b] A_2	A_4	Placement	Comment
702.0	90 ± 3	102 ± 6[e]	0.22 ± 0.03	0.08 ± 0.04	1572 4+ → 870 2+	
727.4	5.1 ± 0.5	prompt	0.17 ± 0.08	0.04 ± 0.12	(2300 → 1572 4+)	placement probable, coinc.
755.9	7.3 ± 0.5	prompt	0.27 ± 0.13	-0.02 ± 0.19	3364(7-) → 2608(5-)	
848.9	69 ± 3	117 ± 6[e]	0.18 ± 0.05	0.13 ± 0.07	2421 6+ → 1572 4+	
870.2	100	111 ± 6[e]	0.20 ± 0.06	0.09 ± 0.09	870 2+ → gs, 0+	
911.6	3.0 ± 0.5	prompt[c]	0.47 ± 0.11	-0.21 ± 0.16	(3865 → 2953 8±)	placement probable, del. coinc.
936.3	8.8 ± 0.8	prompt	0.18 ± 0.08	-0.20 ± 0.12	3357(8+) → 2421 6+	
941.3	29 ± 1	prompt[c]	0.20 ± 0.04	0.03 ± 0.06	3894(10±) → 2953 8±	
981.9	2.8 ± 0.4	prompt[c]				probably ^{94}Mo, del. coinc.
1035.8	11.3 ± 0.6	prompt	-0.36 ± 0.05	-0.03 ± 0.08	2608(5-) → 1572 4+	
1052.3	3.5 ± 0.5	prompt[c]	-0.87 ± 0.15	0.18 ± 0.31	4005 → 2953 8±	
1166.3	5.2 ± 0.5	prompt			(2738(4+) → 1572 4+)	placement probable, coinc.
1868.9	2.2 ± 0.6	prompt			(2738(4+) → 870 2+)	placement probable, energy diff.

[a] Total prompt + delayed intensity.

[b] Angular distributions measured in an ≈ 20 ns wide prompt time window. Distributions of delayed (109 ns) components are totally attenuated.

(continued)

Table 3. (Continued)

[c] Transition precedes isomeric state.

[d] Measured from the relative intensities in the delayed cascade 84 - 449 keV.

[e] Plus a prompt component (very weak in the case of the 449-keV γ ray).

Table 4. γ rays from the reaction $^{94}Zr(\alpha,2n\gamma)^{96}Mo$

E_γ(keV)	I_γ Relative	Angular Distribution A_2	Angular Distribution A_4	Placement	Comment
170.9	1.7 ± 0.2	-0.12 ± 0.06	0.14 ± 0.09		probably ^{96}Mo, coinc.
241.6	0.76 ± 0.20			1869 4+ → 1628 4+	
434.8	2.8 ± 0.6				probably ^{96}Mo, coinc.
460.5	2.2 ± 0.5			2439 5+ → 1978 3+	
538.2	30 ± 2	0.34 ± 0.05	0.04 ± 0.07	2979 8+ → 2441 6+	
546.2	8.2 ± 1.0	-0.23 ± 0.05	0.19 ± 0.08	3916 → 3370(8+)	
569.1	4.0 ± 1.0	-0.55 ± 0.13	-0.09 ± 0.22	2439 5+ → 1869 4+	
719.9	3.5 ± 0.8			1498 2+ → 778 2+	
738.7	2.1 ± 0.8			(3473 → 2734(5-))	placement probable, coinc.
745.9	3.7 ± 0.8	-0.47 ± 0.11	-0.25 ± 0.20	4533 → 3787(10+)	
778.3	100	0.32 ± 0.03	0.12 ± 0.04	778 2+ → gs 0+	
796.8	2.9 ± 0.8			4584 → 3787(10+)	
802.4	2.7 ± 0.6				assignm. uncertain
808.6	16 ± 2	0.52 ± 0.06	-0.12 ± 0.09	3787(10+) → 2979 8+	
812.6	61 ± 3	0.36 ± 0.04	-0.02 ± 0.06	2441 6+ → 1628 4+	
849.8	80 ± 3	0.37 ± 0.04	0.00 ± 0.05	1628 4+ → 778 2+	
858.5	2.8 ± 0.8				assignm. uncertain

(continued)

Table 4. (Continued)

E_γ(keV)	I_γ Relative	Angular Distribution A_2	A_4	Placement	Comment
863.3	1.7 ± 0.8				assignm. uncertain
875.2	2.6 ± 0.7				assignm. uncertain
879.3	4.8 ± 0.8	0.22 ± 0.15	-0.08 ± 0.25	4795 → 3916	
886.1	2.7 ± 1.2				assignm. uncertain
896.9	1.4 ± 0.7				assignm. uncertain
929.3	16 ± 1	0.36 ± 0.07	-0.06 ± 0.11	3370(8+) → 2441 6+	
1006.3	2.8 ± 0.8			(3445 → 2439 5+)	placement probable, coinc.
1032.2	2.7 ± 0.7			(3473 → 2441 6+)	placement probable, coinc.
1055.1	2.4 ± 0.9				probably ^{96}Mo, coinc.
1091.2	8.9 ± 0.9	0.15 ± 0.15	0.01 ± 0.24	1869 4+ → 778 2+	
1105.8	4.2 ± 1.0	-0.31 ± 0.14	0.14 ± 0.22	2734(5-) → 1628 4+	
1125.6	4.2 ± 0.9	0.09 ± 0.17	0.12 ± 0.24	2754 6+ → 1628 4+	
1136.9	0.9 ± 0.6				assignm. uncertain
1138.2	1.0 ± 0.5				assignm. uncertain
1171.8	1.9 ± 0.7				assignm. uncertain
1200.1	3.4 ± 1.0			1978 3+ → 778 2+	

Table 5. γ rays from the reaction $^{96}Zr(\alpha,2n\gamma)^{98}Mo$

E_γ(keV)	I_γ Relative	Angular Distribution A_2	Angular Distribution A_4	Placement	Comment
129.2	0.38 ± 0.07				probably ^{98}Mo, coinc.
157.8	1.15 ± 0.12			2837 → 2679(5,6+)	
169.4	1.57 ± 0.16			(4610 → 4441)	placement probable, coinc.
173.2	1.53 ± 0.16				probably ^{98}Mo, coinc.
227.3	1.27 ± 0.14			(2571 → 2344 6+)	placement probable, coinc.
241.7	1.0 ± 0.5			(3096(7-) → 2854[8+])	placement probable, coinc.
259.0?	1.26 ± 0.20				possibly in ^{97}Mo
282.2	0.5 ± 0.3			(2854[8+] → 2571)	placement possible, energy diff.
290.8	1.9 ± 0.3			(4441 → 4150[10+])	placement probable, coinc.
335.1	1.57 ± 0.20			2679(5,6+) → 2344 6+	
385.1	3.9 ± 0.3			3657(9-) → 3272 8+	
394.4	4.3 ± 0.3			(2738 → 2344 6+)	placement probable coinc.
431.7	2.1 ± 0.3				probably ^{98}Mo, coinc.
475.7	9.3 ± 0.5	0.24 ± 0.14	-0.12 ± 0.20	3096(7-) → 2621(5-)	
510.5[a]	14 ± 2[a]			2854[8+] → 2344 6+	
560.7	5.4 ± 0.4[b]			3657(9-) → 3096(7-)	

(continued)

Table 5. (Continued)

E_γ(keV)	I_γ Relative	Angular Distribution A_2	A_4	Placement	Comment
603.5	5.2 ± 0.5			2621(5-) → 2017(3-)	
644.6	1.6 ± 0.5			1432 2+ → 788 2+	known transition in ^{98}Mo
662.8	3.2 ± 0.8				probably ^{98}Mo, coinc.
672.6	7.8 ± 0.5			3769[9-] → 3096(7-)	
722.8[c]	85 ± 4[c]	0.18 ± 0.05	-0.09 ± 0.07	1510 4+ → 788 2+	
752.8[d]	12 ± 3[d]			3096(7-) → 2344 6+	
767.2	5.1 ± 0.8			4424 → 3657(9-)	
769.1	4.5 ± 0.8			4538 → 3769[9-]	
787.6	100	0.16 ± 0.03	-0.09 ± 0.06	788 2+ → gs 0+	
833.7	57 ± 2	0.20 ± 0.04	-0.10 ± 0.06	2344 6+ → 1510 4+	
878.1	5.4 ± 0.5			4150[10+] → 3272 8+	
892.3	3.7 ± 0.6				probably ^{98}Mo, coinc.
898.1	3.9 ± 0.6				probably ^{98}Mo, coinc.
928.1	18 ± 1	0.21 ± 0.07	-0.18 ± 0.11	3272 8+ → 2344 6+	
1110.4	10.9 ± 0.7	-0.18 ± 0.10	0.00 ± 0.15	2621(5-) → 1510 4+	
1168.2	3.6 ± 0.6			2679(5,6+) → 1510 4+	
1229.7	6.9 ± 0.8			2017(3-) → 788 2+	

(continued)

Table 5. (Continued)

[a]Not annihilation radiation. Intensity derived from the coincidence spectra.

[b]Part of the intensity of this line may belong to an unresolved transition, possibly in ^{97}Mo.

[c]According to the coincidence results, this γ ray masks a γ ray at 723.1 keV in ^{97}Mo. The intensity is corrected for a 10% contribution from the latter transition.

[d]From the coincidence spectra. This γ ray is masked in the singles spectrum by a 751.9-keV transition in ^{97}Mo.

Table 6. γ rays from the reaction $^{94}Mo(\alpha,2n\gamma)^{96}Ru$

E_γ, keV	I_γ Relative	Angular Distribution A_2	Angular Distribution A_4	Placement	Comment
112.4	1.1 ± 0.2	0.05 ± 0.05	0.02 ± 0.07	4711 → 4598	
180.1	1.1 ± 0.2			4598 → 4418(12+)	
264.7	0.9 ± 0.2			(4082 → 3817(10+))	placement possible, coinc.
274.3	0.8 ± 0.2			(3817(10+) → 3543)	placement probable, energy diff.
292.3	0.9 ± 0.2			4711 → 4418(12+)	
336.2	1.4 ± 0.2	0.05 ± 0.09	-0.11 ± 0.16	4598 → 4262[12+]	
352.7	0.8 ± 0.2				probably ^{96}Ru, excit.
372.7	1.3 ± 0.3				probably ^{96}Ru, excit.
445.3	5.2 ± 0.5	0.37 ± 0.07	-0.13 ± 0.11	4262[12+] → 3817(10+)	
448.2	2.0 ± 0.3			4711 → 4262[12+]	
497.9	2.0 ± 0.4			(5096 → 4598)	placement possible, coinc.
526.3	2.5 ± 0.4	-0.25 ± 0.14	0.15 ± 0.23		probably ^{96}Ru, excit.
537.9	1.4 ± 0.3				probably ^{96}Ru, excit.
583.3	5.0 ± 0.5	0.04 ± 0.08	-0.22 ± 0.15	(4534 → 3951(9-))	placement possible, coinc.
593.7	3.5 ± 0.5	0.31 ± 0.14	0.07 ± 0.21	(3543 → 2950 8+)	placement probable, coinc.
600.9	9.9 ± 0.8	0.40 ± 0.10	-0.04 ± 0.15	4418(12+) → 3817(10+)	
631.8	58 ± 2	0.37 ± 0.03	-0.05 ± 0.04	2150 6+ → 1518 4+	

(continued)

Table 6. (Continued)

E_γ, keV	I_γ Relative	Angular Distribution A_2	A_4	Placement	Comment
644.1	2.2 ± 0.4			1477 2+ → 832 2+	
652.3	1.0 ± 0.4			(3543 → 2891)	placement probable, coinc.
659.7	13.6 ± 0.6	0.37 ± 0.06	-0.15 ± 0.09	3951(9-) → 3291 7(-)	
685.5	95 ± 3	0.36 ± 0.04	-0.12 ± 0.07	1518 4+ → 832 2+	
703.0	19 ± 2	0.28 ± 0.07	0.03 ± 0.11	3291 7(-) → 2588 5(-)	
741.3	2.2 ± 0.5			(2891 → 2150 6+)	placement probable, coinc.
745.4	1.8 ± 0.4				probably ^{96}Ru, excit.
800.7	36 ± 1	0.34 ± 0.04	-0.11 ± 0.06	2950 8+ → 2150 6+	
832.5	100	0.33 ± 0.04	-0.09 ± 0.07	832 2+ → gs 0+	
848.0	5.3 ± 0.5			(4799 → 3951(9-))	placement possible, coinc.
866.7	23 ± 1	0.36 ± 0.06	-0.06 ± 0.09	3817(10+) → 2950 8+	
892.8	1.9 ± 0.5				probably ^{96}Ru, excit.
927.0	4.0 ± 0.5				probably ^{96}Ru, excit.
995.6	3.7 ± 0.5				^{96}Ru or ^{97}Ru
1000.0	3.3 ± 0.5			3951(9-) → 2950 8+	
1070.2	24 ± 1	-0.25 ± 0.05	-0.09 ± 0.08	2588 5(-) → 1518 4+	
1097.7	2.1 ± 0.5				probably ^{96}Ru, coinc.

(continued)

Table 6. (Continued)

E_γ,keV	I_γ Relative	Angular Distribution A_2	A_4	Placement	Comment
1393.7	3.3 ± 0.5			(3543 → 2150 6+)	placement probable, energy diff.
1476.8	1.9 ± 0.5			1477 2+ → gs 0+	

Table 7. γ rays observed in the reaction $^{96}Mo(\alpha,2n\gamma)^{98}Ru$

E_γ,keV	I_γ Relative	Angular Distribution A_2	A_4	Placement	Comment
253.7	1.4 ± 0.2	-0.37 ± 0.11	0.01 ± 0.19	2266(5,6) → 2013(3,4)	
382.9	1.9 ± 0.3	-0.12 ± 0.08	-0.06 ± 0.13	1797(3,4) → 1414 2+	
469.9	5.8 ± 0.4	0.73 ± 0.14	0.06 ± 0.18	2266(5,6) → 1797(3,4)	
598.9	2.5 ± 0.4			2013(3,4) → 1414 2+	
615.2	2.6 ± 0.4			2013(3,4) → 1398 4+	
652.7	100	0.36 ± 0.03	0.04 ± 0.05	653 2+ → gs 0+	
722.6	2.8 ± 0.5			(4006 → 3284)	placement probable,coinc.
724.9	7.1 ± 0.4	-0.20 ± 0.08	0.12 ± 0.13	3852(9-) → 3127 8+	
745.6	81 ± 3	0.35 ± 0.03	-0.02 ± 0.04	1398 4+ → 653 2+	
762.0	4.0 ± 0.4			1414 2+ → 653 2+	
810.8	3.1 ± 0.4			(4001(10+) → 3190(8+))	placement probable,coinc.
820.7	4.7 ± 0.4	0.37 ± 0.07	-0.11 ± 0.09	4672 → 3852(9-)	
824.9	57 ± 2	0.30 ± 0.03	-0.09 ± 0.05	2223 6+ → 1398 4+	
862.9	2.2 ± 0.4				assignm. uncertain
868.6	1.6 ± 0.3			(2266(5,6) → 1398 4+)	placement possible, energy diff.
874.5	7.3 ± 0.4	0.52 ± 0.08	0.01 ± 0.09	4001(10+) → 3127 8+	
904.0	26 ± 1	0.38 ± 0.04	-0.02 ± 0.05	3127 8+ → 2223 6+	

(continued)

Table 7. (Continued)

E_γ, keV	I_γ Relative	Angular Distribution A_2	A_4	Placement	Comment
967.8	14.2 ± 0.6	0.47 ± 0.06	0.04 ± 0.09	3190(8+) → 2223 6+	
1032.7	4.3 ± 0.5	0.39 ± 0.13	-0.19 ± 0.19	(3255 → 2223 6+)	placement probable, coinc.
1061.1	6.1 ± 0.5	-0.01 ± 0.15	-0.05 ± 0.23	3284 → 2223 6+	
1143.9	8.1 ± 0.6			1797(3,4) → 653 2+	
1148.5	7.3 ± 0.6			2546(5,6) → 1398 4+	
1257.9	4.9 ± 0.5			2656(5,6) → 1398 4+	
1414.0	2.2 ± 0.5			1414 2+ → gs 0+	

Table 8. γ rays from the reaction $^{98}Mo(\alpha,2n\gamma)^{100}Ru$

E_γ(keV)	I_γ Relative	Angular Distribution A_2	A_4	Placement	Comment
91.7?	0.13 ± 0.03			[3357 → 3266]	assignm. uncertain
148.8	1.13 ± 0.11			3507(9-) → 3357	
187.6	1.54 ± 0.15			3142[7-] → 2954(7-)	
203.4	1.40 ± 0.13			3266 → 3063 8+	
294.8?	0.41 ± 0.15			[3357 → 3063 8+]	assignm. uncertain
364.5	2.6 ± 0.3	0.45 ± 0.10	0.00 ± 0.15	3507(9-) → 3142[7-]	
391.5	5.4 ± 0.4	0.50 ± 0.06	0.12 ± 0.09	3357 → 2966	
403.6	3.4 ± 0.3	0.69 ± 0.20	0.24 ± 0.26	3357 → 2954(7-)	
418.1?	0.8 ± 0.2				assignm. uncertain
424.7	3.5 ± 0.3	0.35 ± 0.10	0.07 ± 0.15	2954(7-) → 2529(5-)	
431.2?	0.9 ± 0.3				assignm. uncertain
437.2	2.0 ± 0.3			2966 → 2529(5-)	
443.9	3.2 ± 0.3	-0.34 ± 0.15	0.05 ± 0.23	3507(9-) → 3063 8+	
464.9	1.4 ± 0.7			(2529(5-) → 2064(3-,4+)	placement probable, coinc.
489.4	2.2 ± 0.3	0.29 ± 0.15	0.26 ± 0.20		probably ^{100}Ru, coinc.
540.2	100	0.32 ± 0.02	-0.07 ± 0.03	540 2+ → gs 0+	
552.5	4.5 ± 0.3	0.61 ± 0.13	-0.04 ± 0.18	3507(9-) → 2954(7-)	

(continued)

Table 8. (Continued)

E_γ(keV)	I_γ Relative	Angular Distribution A_2	A_4	Placement	Comment
591.5	0.9 ± 0.4			1132 0+ → 540 2+	known transition in ^{100}Ru
612.7	2.6 ± 0.3			3142[7-] → 2529(5-)	
624.5	8.3 ± 0.5	0.30 ± 0.08	-0.05 ± 0.12	3579(9-) → 2954(7-)	
637.9	6.5 ± 0.5	0.28 ± 0.07	-0.03 ± 0.10	3996 → 3357	
643.5	2.8 ± 0.4				probably ^{100}Ru, coinc.
648.4	1.8 ± 0.3				probably ^{100}Ru, coinc.
687.6	86 ± 3	0.29 ± 0.02	-0.06 ± 0.03	1228 4+ → 540 2+	
701.2?	3.9 ± 0.5				possibly ^{100}Ru, excit.
710.5	3.1 ± 0.6				possibly ^{100}Ru, excit.
728.0	5.8 ± 0.4	0.29 ± 0.17	0.12 ± 0.25	4235 → 3507(9-)	
740.8	4.5 ± 0.4	0.78 ± 0.43	0.15 ± 0.78	4320 → 3579(9-)	
793.2	2.1 ± 0.8				probably ^{100}Ru, coinc., excit.
803.6?	2.7 ± 0.4				possibly ^{100}Ru, excit.
806.9	3.3 ± 0.5			(4803 → 3996)	placement probable, coinc.
823.3	1.8 ± 0.7			1363 2+ → 540 2+	known transition in ^{100}Ru
836.1	4.4 ± 0.5	0.31 ± 0.10	0.06 ± 0.16	(2064(3-,4+) → 1228 4+)	placement probable, coinc.
849.9	63 ± 3	0.29 ± 0.03	-0.12 ± 0.04	2078 6+ → 1228 4+	

(continued)

Table 8. (Continued)

E_γ(keV)	I_γ Relative	Angular Distribution A_2	A_4	Placement	Comment
876.6	19 ± 2	-0.27 ± 0.04	0.00 ± 0.06	2954(7-) → 2078 6+	
888.8	3.8 ± 0.5	0.41 ± 0.08	-0.11 ± 0.11	2966 → 2078 6+	
985.2	25 ± 2	0.35 ± 0.03	-0.11 ± 0.05	3063 8+ → 2078 6+	
1024.1	7.0 ± 0.6	0.45 ± 0.12	-0.26 ± 0.17	4087(10+) → 3063 8+	
1188.1?	1.8 ± 0.6			(3266 → 2078 6+)	placement possible,coinc., energy diff.
1293.7	2.2 ± 0.5				assignm. uncertain
1301.2	10.6 ± 0.9	-0.30 ± 0.10	0.03 ± 0.16	2529(5-) → 1228 4+	
1341.9	2.4 ± 0.6			(1882(3+) → 540 2+)	placement probable,coinc.
1363.5	1.2 ± 0.5			1363 2+ → gs 0+	known transition in ^{100}Ru
1434.8?	1.4 ± 0.6				assignm. uncertain
1479.8?	1.9 ± 0.7				assignm. uncertain
1523.8	2.3 ± 0.6			(2064(3-,4+) → 540 2+)	placement possible, energy diff.
1628.9	1.3 ± 0.5				assignm. uncertain

Table 9. γ rays from the reaction $^{100}Mo(\alpha,2n\gamma)^{102}Ru$

E_γ, keV	I_γ Relative	Angular Distribution A_2	Angular Distribution A_4	Placement	Comment
235.4[a]	4.3 ± 0.3			2942(8-) → 2706(7-) +(2706(7-) → 2471)	
277.1	2.2 ± 0.3			2650(6-) → 2372(5-)	
292.1	7.9 ± 0.4	0.48 ± 0.07	-0.12 ± 0.10	2942(8-) → 2650(6-)	
333.8	4.8 ± 0.3	0.54 ± 0.21	0.26 ± 0.29	2706(7-) → 2372(5-)	
475.7	100	0.29 ± 0.03	-0.06 ± 0.04	476 2+ → gs 0+	
595.7	8.5 ± 0.8	0.18 ± 0.12	0.34 ± 0.20	(2471 → 1875 6+)	
621.5	8.7 ± 0.7	0.24 ± 0.10	-0.36 ± 0.20	4056 → 3434	
628.0	3.3 ± 0.5			1104 2+ → 476 2+	
631.9	85 ± 3	0.28 ± 0.03	-0.08 ± 0.04	1108 4+ → 476 2+	
680.7	7.6 ± 0.7	0.48 ± 0.10	0.20 ± 0.14	3387(9-) → 2706(7-)	
686.0	3.3 ± 0.8				probably ^{102}Ru, excit.
727.6	13.5 ± 0.6	0.44 ± 0.20	0.45 ± 0.28	3434 → 2706(7-)	
767.5	61 ± 2	0.36 ± 0.05	-0.05 ± 0.08	1875 6+ → 1108 4+	
775.2	6.9 ± 0.6	0.56 ± 0.14	0.11 ± 0.19	2650(6-) → 1875 6+	
787.1	2.9 ± 0.6				assignm. uncertain
803.6	2.6 ± 0.6				assignm. uncertain
816.3	4.5 ± 0.8				probably ^{102}Ru, excit.

(continued)

Table 9. (Continued)

E_γ, keV	I_γ Relative	Angular Distribution A_2	A_4	Placement	Comment
831.4	43 ± 2	0.10 ± 0.04	-0.09 ± 0.06	2706(7-) → 1875 6+	
962.4	3.2 ± 0.8				assignm. uncertain
1047.3	5.8 ± 0.8			(2155 → 1108 4+)	placement probable, coinc.
1104.0	2.6 ± 0.8			1104 2+ → gs 0+	
1150.8	2.1 ± 0.6				assignm. uncertain
1264.5	11.1 ± 1.0			2372(5-) → 1108 4+	
1594.3	2.8 ± 0.9				assignm. uncertain

[a] Doublet. See text.

FIGURE CAPTIONS

Fig. 1. Target chamber and γ-ray detectors: configuration used for measurement of angular distributions. The inset shows the last part of the beam-line.

Fig. 2. Simplified block diagram of the electronic circuitry for measuring energies, intensities, and lifetimes of γ-rays.

Fig. 3. Level schemes for ^{92}Mo and ^{94}Ru. Only levels and transitions observed in the present study are shown. The numbers next to arrows at the right side of the level scheme are the "unaccounted feeding" in percent; that is, they represent the feeding by neutron emission and γ-ray transitions which were not resolved or placed in the scheme. The same comments apply to figs. 4-10.

Fig. 4. Level scheme of ^{94}Mo.

Fig. 5. Level scheme of ^{96}Mo.

Fig. 6. Level scheme of ^{98}Mo.

Fig. 7. Level scheme of ^{96}Ru.

Fig. 8. Level scheme of ^{98}Ru.

Fig. 9. Level scheme of ^{100}Ru

Fig. 10. Level scheme of ^{102}Ru.

Fig. 11. Comparison of the known levels of ^{94}Mo and ^{96}Mo with shell-model calculations[65,66]).

Fig. 12. Systematics of the even-parity states.

Fig. 13. Systematics of the odd-parity states.

Fig. 14. Comparison of the observed quasi-rotational bands with the VMI-model predictions. The VMI calculations for the magic region (dashed lines) follow the prescription of Mariscotti[70]).

Fig. 15. Angular-momentum distribution at various stages of the reaction ^{98}Mo(28-MeV α,2n)^{100}Ru. The solid curve shows the distribution in ^{102}Ru* after absorption of the α particle, calculated from an optical model[75]). The dashed and dot-dashed curves represent the distribution after emission of two neutrons, calculated with a microscopic evaporation model[76]), for two values of the moment-of-inertia parameter $\mathfrak{J}$. The histogram represents the experimental distribution in ^{100}Ru prior to the emission of those γ rays that are placed in the level scheme (fig. 9).

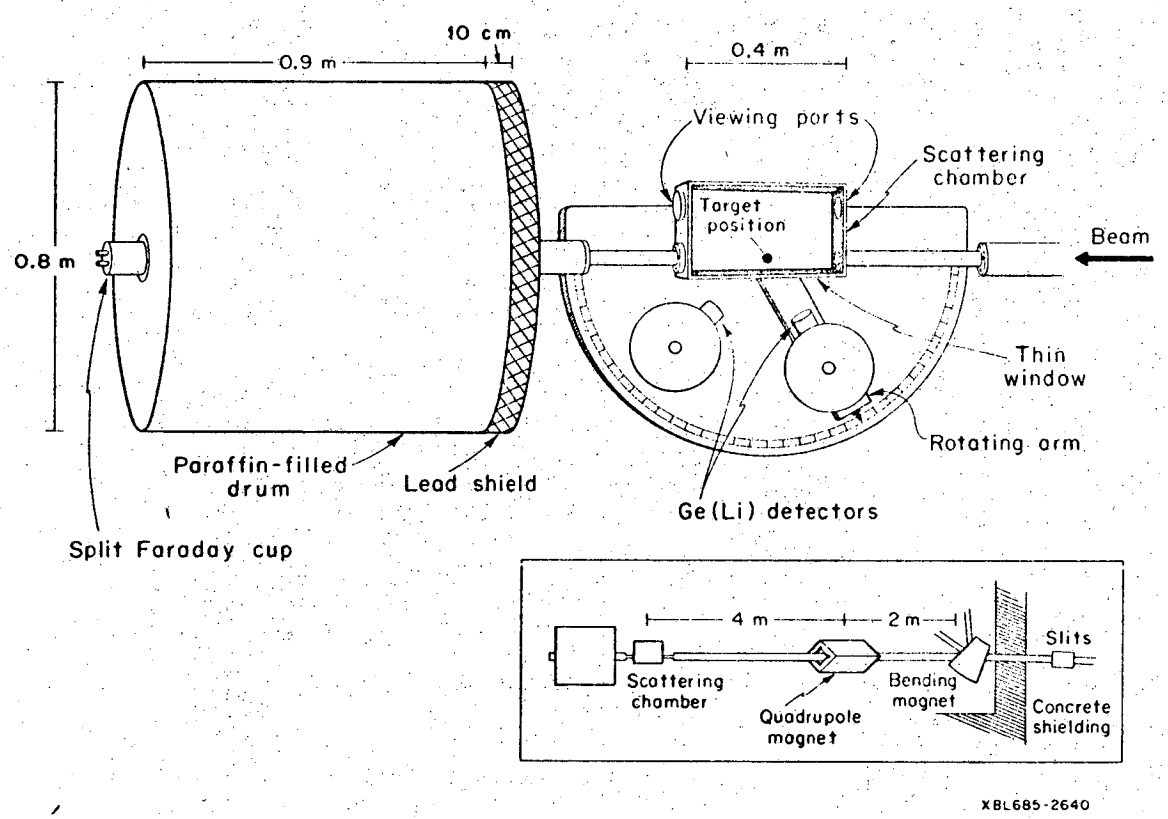
10 cm
0.9 m
0.4 m
Viewing ports
Scattering chamber
Target position
Beam
0.8 m
Thin window
Rotating arm
Paraffin-filled drum
Lead shield
Ge(Li) detectors
Split Faraday cup
4 m
2 m
Slits
Scattering chamber
Bending magnet
Quadrupole magnet
Concrete shielding
XBL685-2640

Fig. 1

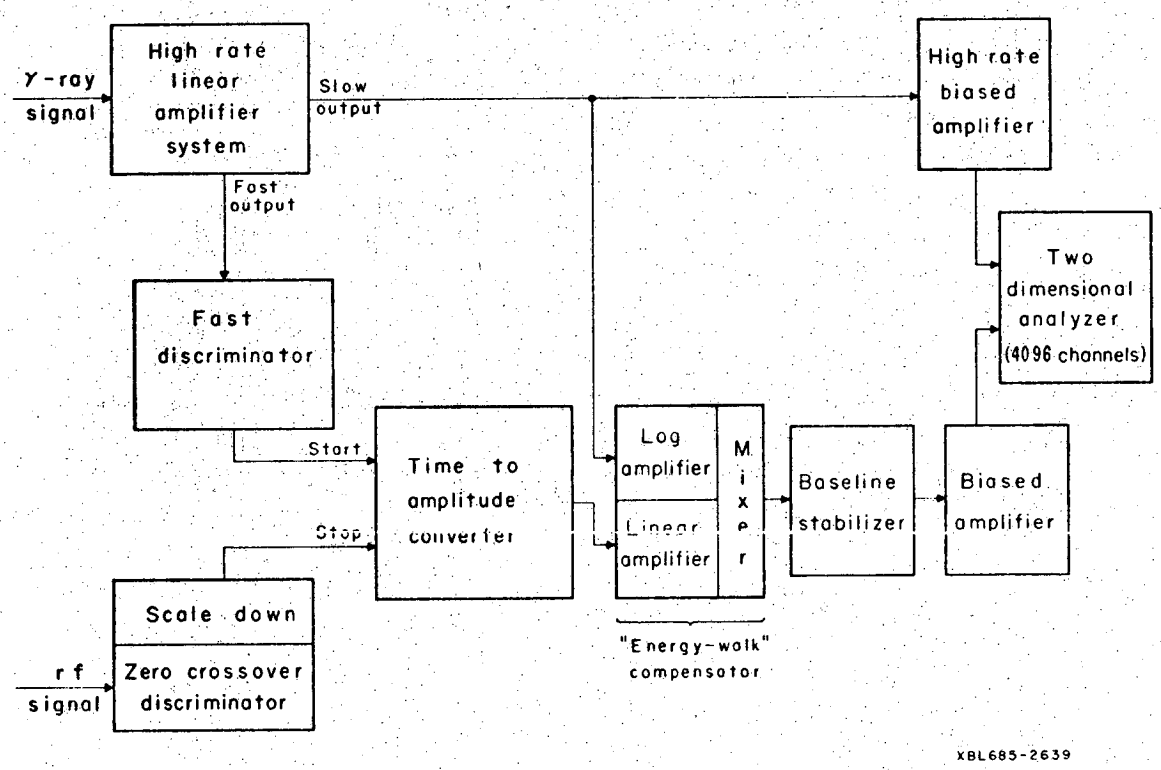
γ-ray signal
High rate linear amplifier system
Slow output
Fast output
High rate biased amplifier
Two dimensional analyzer (4096 channels)
Fast discriminator
Start
Time to amplitude converter
Log amplifier
Linear amplifier
Mixer
Baseline stabilizer
Biased amplifier
Stop
Scale down
Zero crossover discriminator
rf signal
"Energy-walk" compensator
XBL685-2639

Fig. 2

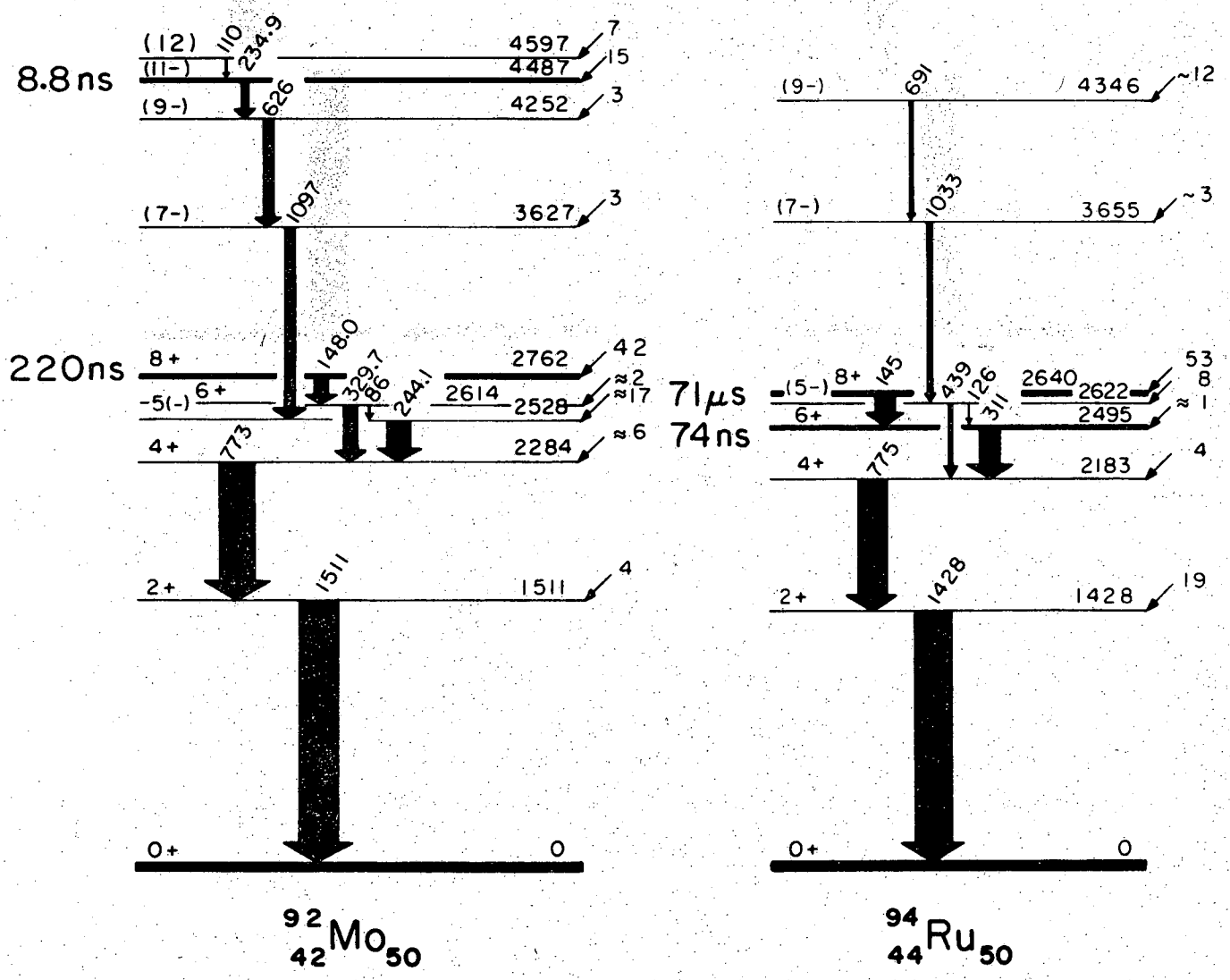

XBL7010-3953

Fig. 3

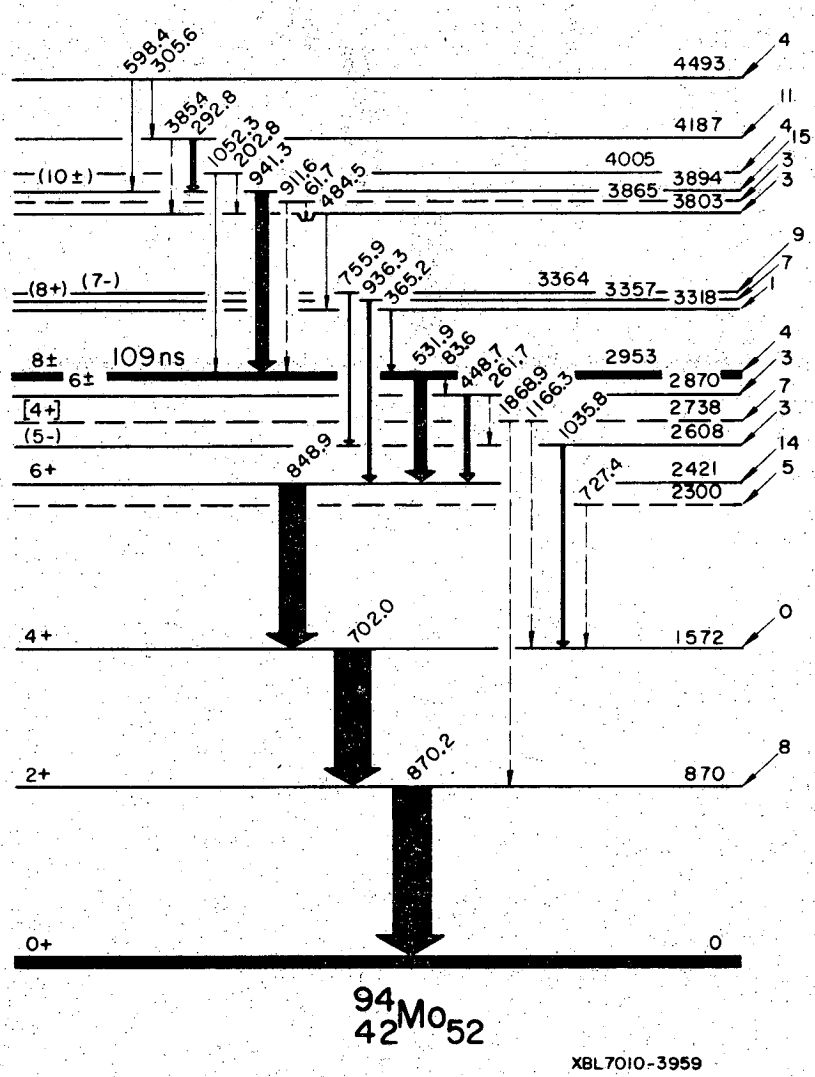
598.4
305.6
4493
4
3854
292.8
1052.3
202.8
4187
11
4
15
941.3
911.6
61.7
484.5
4005
3894
3865
3803
3
3
(10±)
755.9
936.3
365.2
3364
3357
3318
9
7
1
(8+)
(7-)
8±
109 ns
6±
531.9
83.6
448.7
261.7
1868.9
1166.3
2953
2870
2738
2608
4
3
7
3
[4+]
(5-)
1035.8
848.9
6+
727.4
2421
2300
14
5
4+
702.0
1572
0
2+
870.2
870
8
0+
0
$^{94}_{42}Mo_{52}$
XBL7010-3959

Fig. 4

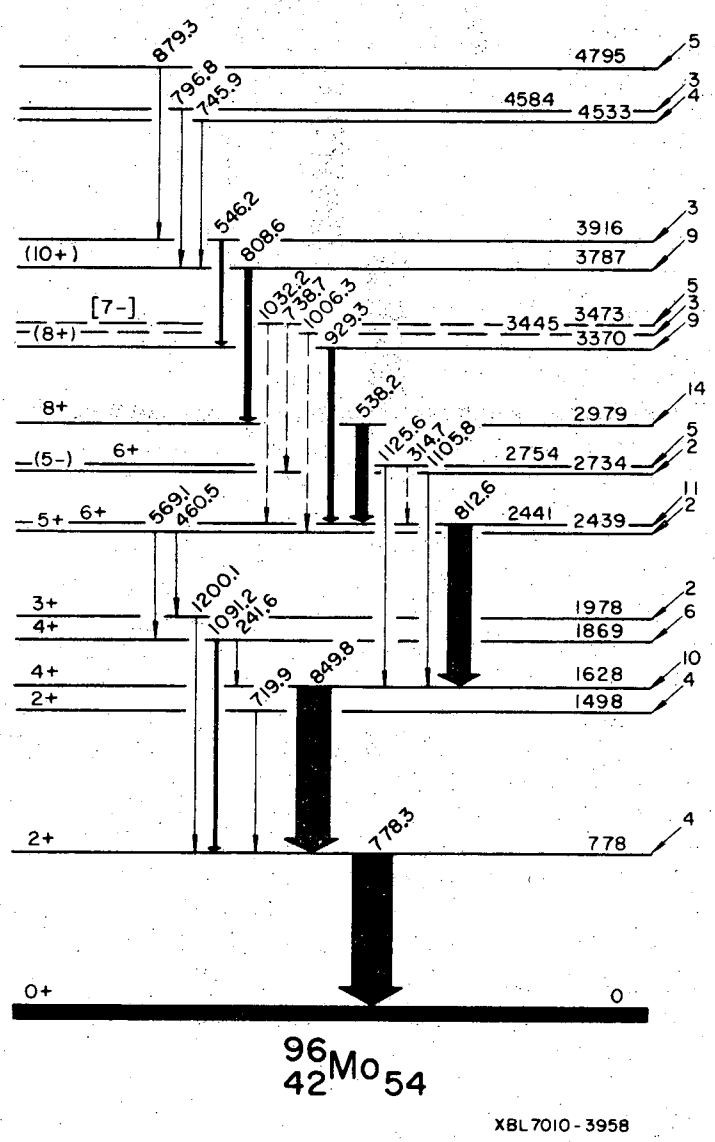
879.3
796.8
745.9
4795
4584
4533
546.2
808.6
3916
3787
(10+)
[7-]
(8+)
1032.2
738.7
1006.3
929.3
3445
3473
3370
8+
538.2
2979
(5-)
6+
1125.6
314.7
1105.8
2754
2734
5+
6+
569.1
460.5
812.6
2441
2439
3+
4+
1200.1
1091.2
241.6
1978
1869
4+
2+
719.9
849.8
1628
1498
2+
778.3
778
0+
0
96 42 Mo 54
XBL7010-3958

Fig. 5

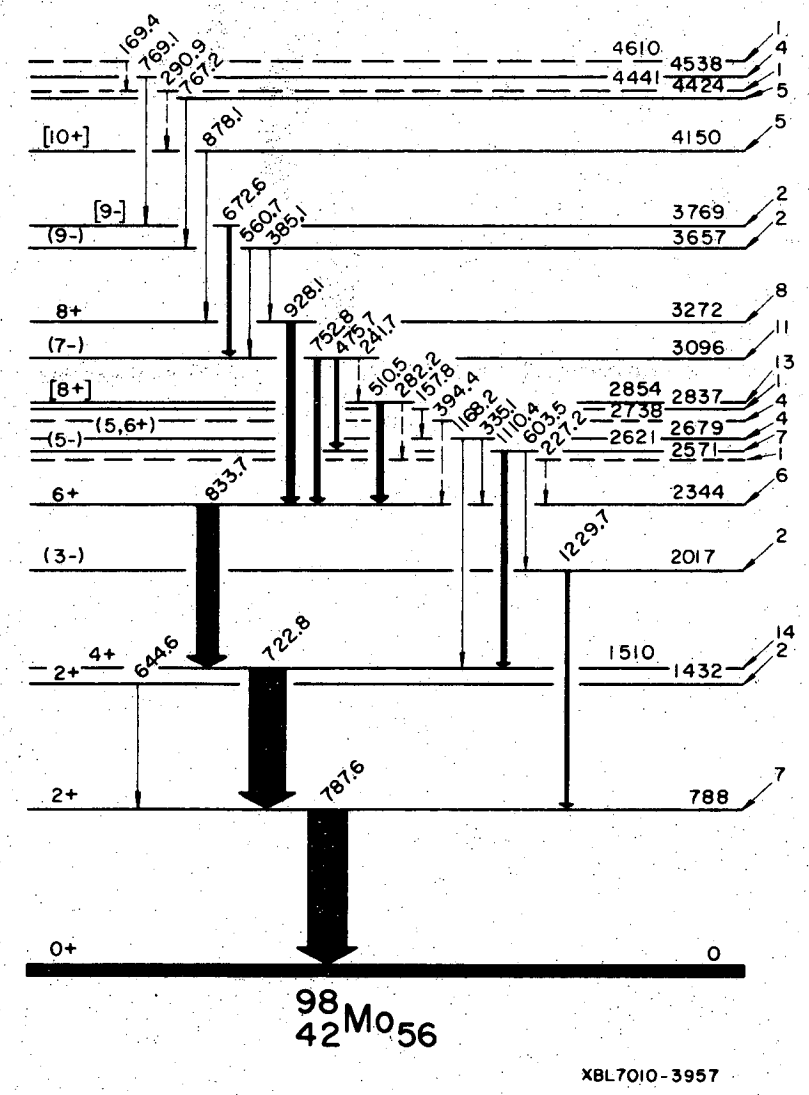
169.4
769.1
290.9
767.2
4610
4538
4441
4424
[10+]
878.1
4150
[9-]
672.6
560.7
385.1
3769
(9-)
3657
8+
928.1
3272
752.8
479.7
241.7
(7-)
3096
[8+]
510.5
282.2
157.8
394.4
168.2
335.1
110.4
603.5
227.2
2854
2837
2738
(5,6+)
2679
(5-)
2621
2571
6+
833.7
2344
(3-)
1229.7
2017
4+
644.6
722.8
1510
2+
1432
2+
787.6
788
0+
0
98
42Mo56
XBL7010-3957

Fig. 6

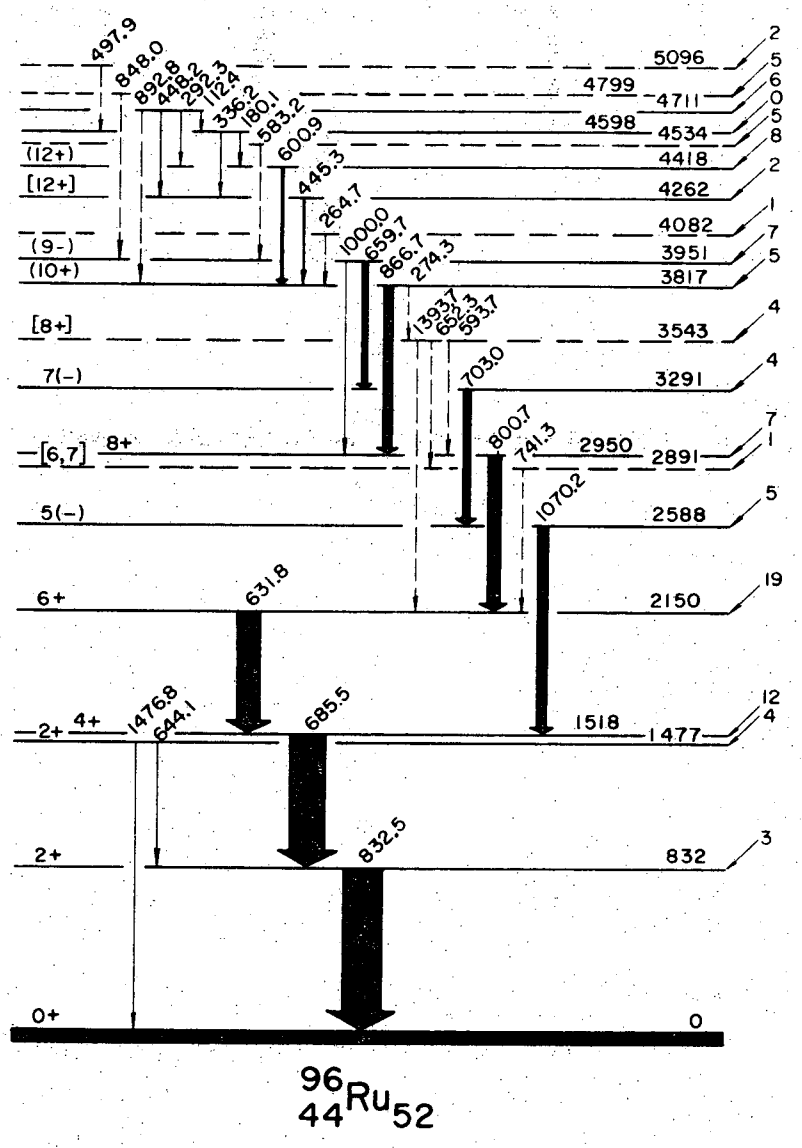

$^{96}_{44}Ru_{52}$

XBL7010-3956

Fig. 7

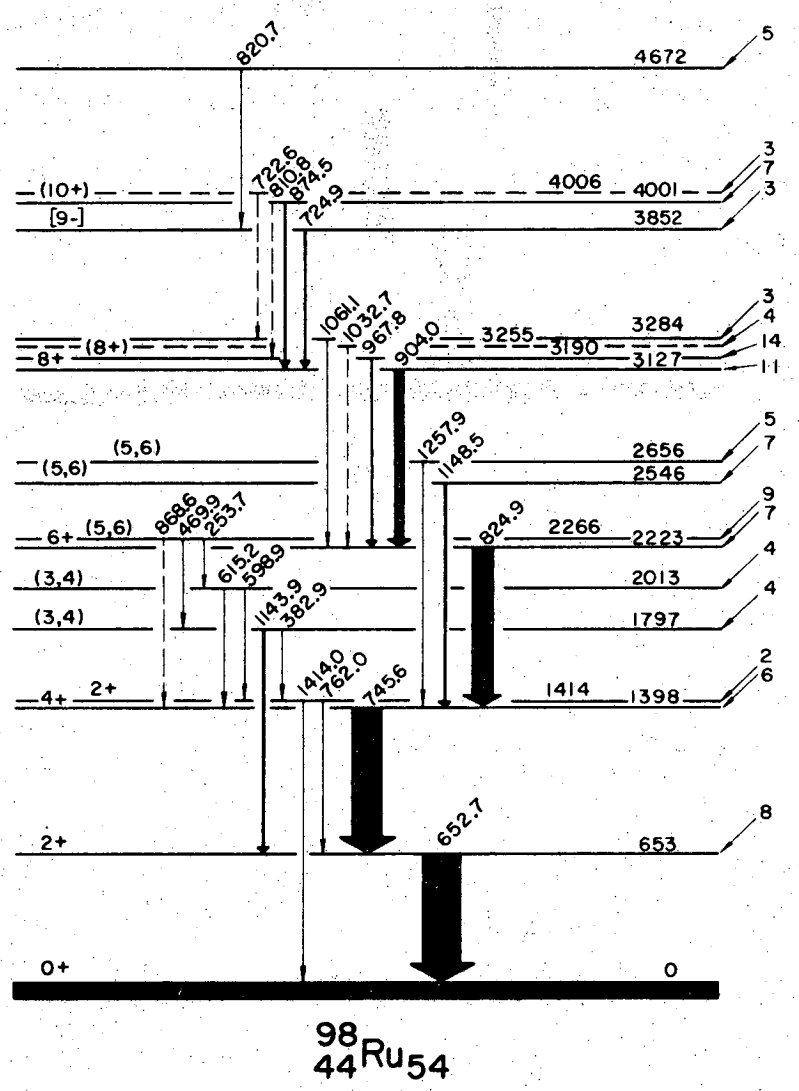
820.7
4672
5
722.6
810.8
874.5
(10+)
4006
4001
3
7
3
[9-]
724.9
3852
1061.1
1032.7
967.8
904.0
3255
3190
3284
3
4
14
11
8+
(8+)
3127
1257.9
1148.5
(5,6)
(5,6)
2656
2546
5
7
868.6
469.9
253.7
6+
(5,6)
824.9
2266
2223
9
7
615.2
598.9
(3,4)
2013
4
1143.9
382.9
(3,4)
1797
4
1414.0
762.0
745.6
4+
2+
1414
1398
2
6
652.7
2+
653
8
0+
0
98
44Ru54
XBL7010-3955

Fig. 8

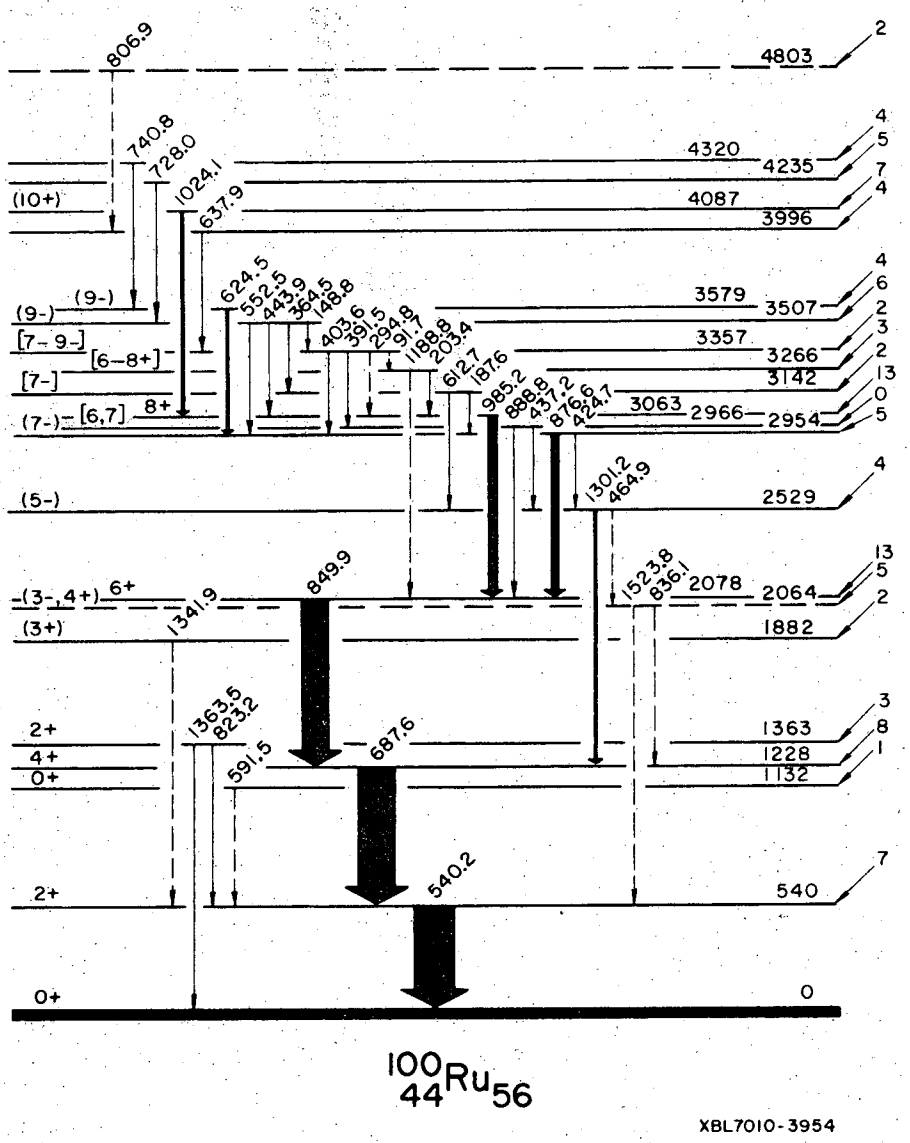
806.9
4803
2
740.8
728.0
1024.1
637.9
4320
4235
4087
3996
(10+)
(9-)
(9-)
[7-9-]
[6-8+]
[7-]
(7-)
[6,7]
8+
624.5
552.5
443.9
364.5
348.8
403.6
391.5
294.8
91.7
1188.8
203.4
61.2
187.6
985.2
888.8
437.2
876.6
424.7
3579
3507
3357
3266
3142
3063
2966
2954
(5-)
1301.2
464.9
2529
(3-,4+)
6+
1341.9
849.9
1523.8
836.1
2078
2064
(3+)
1882
2+
4+
0+
1363.5
823.2
591.5
687.6
1363
1228
1132
2+
540.2
540
0+
0
$^{100}_{44}Ru_{56}$
XBL7010-3954

Fig. 9

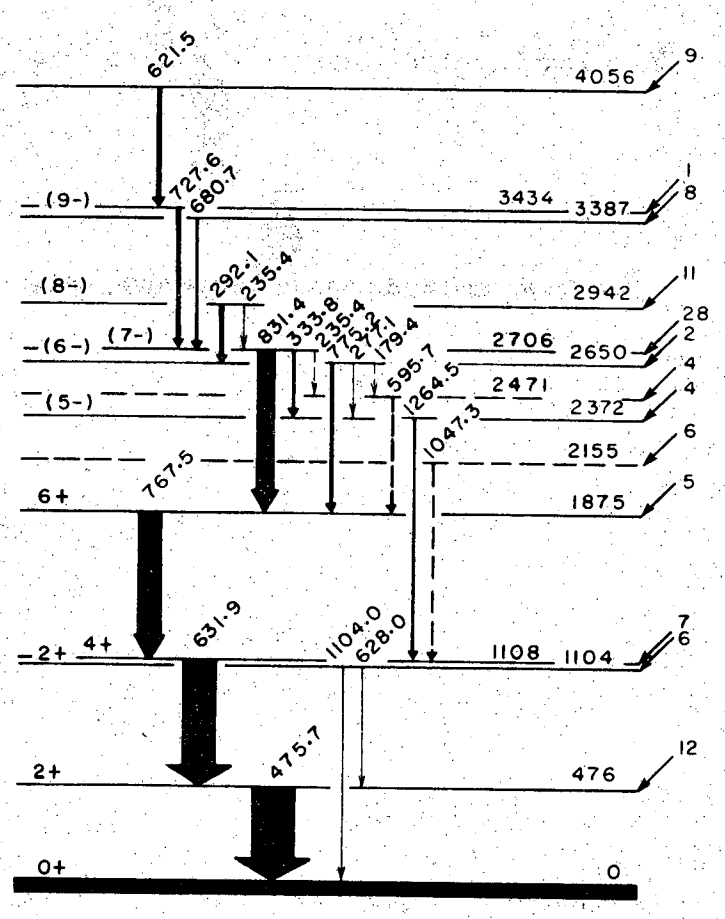

$^{102}_{44}Ru_{58}$

XBL7010-3952

Fig. 10

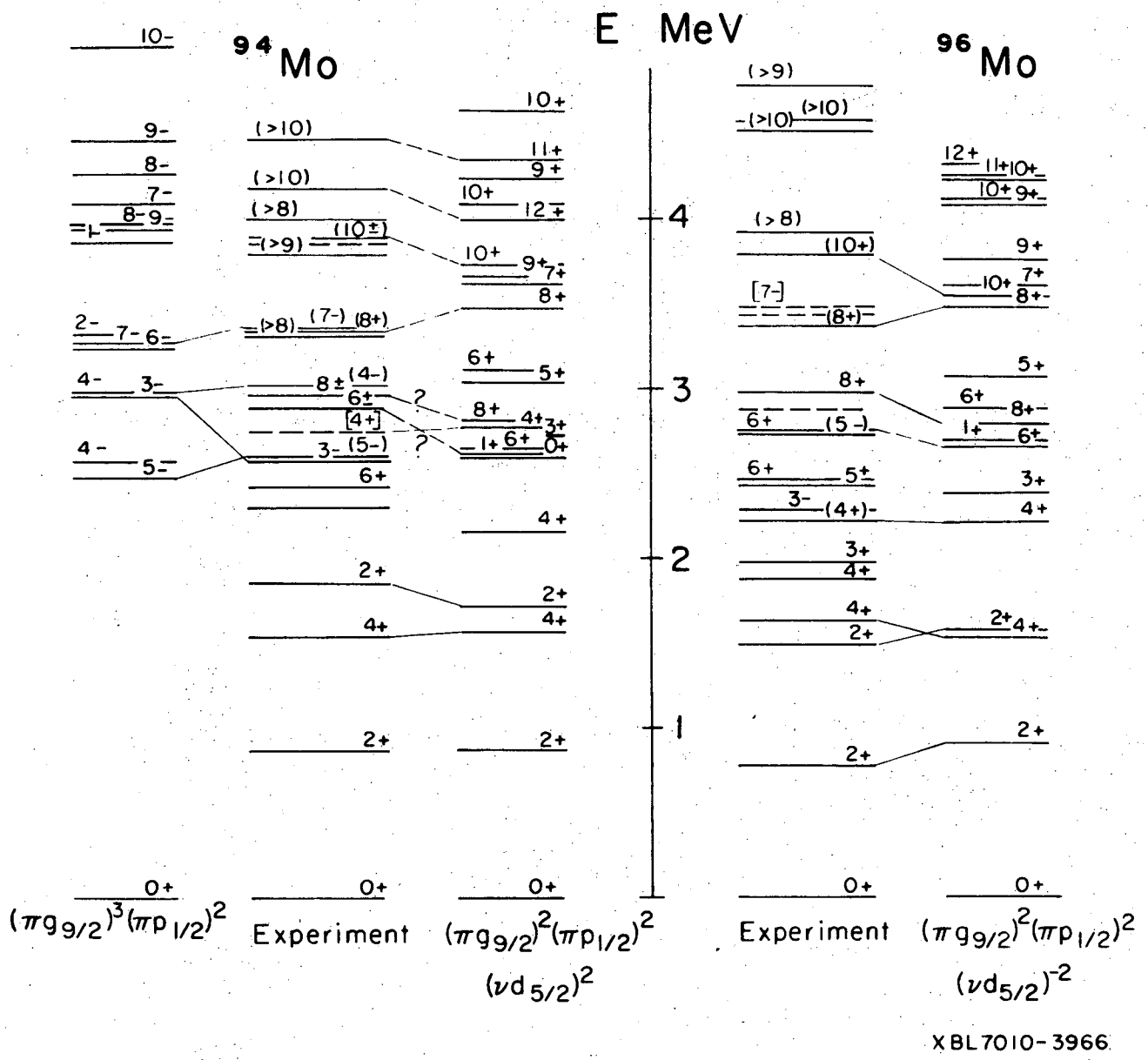

Fig. 11

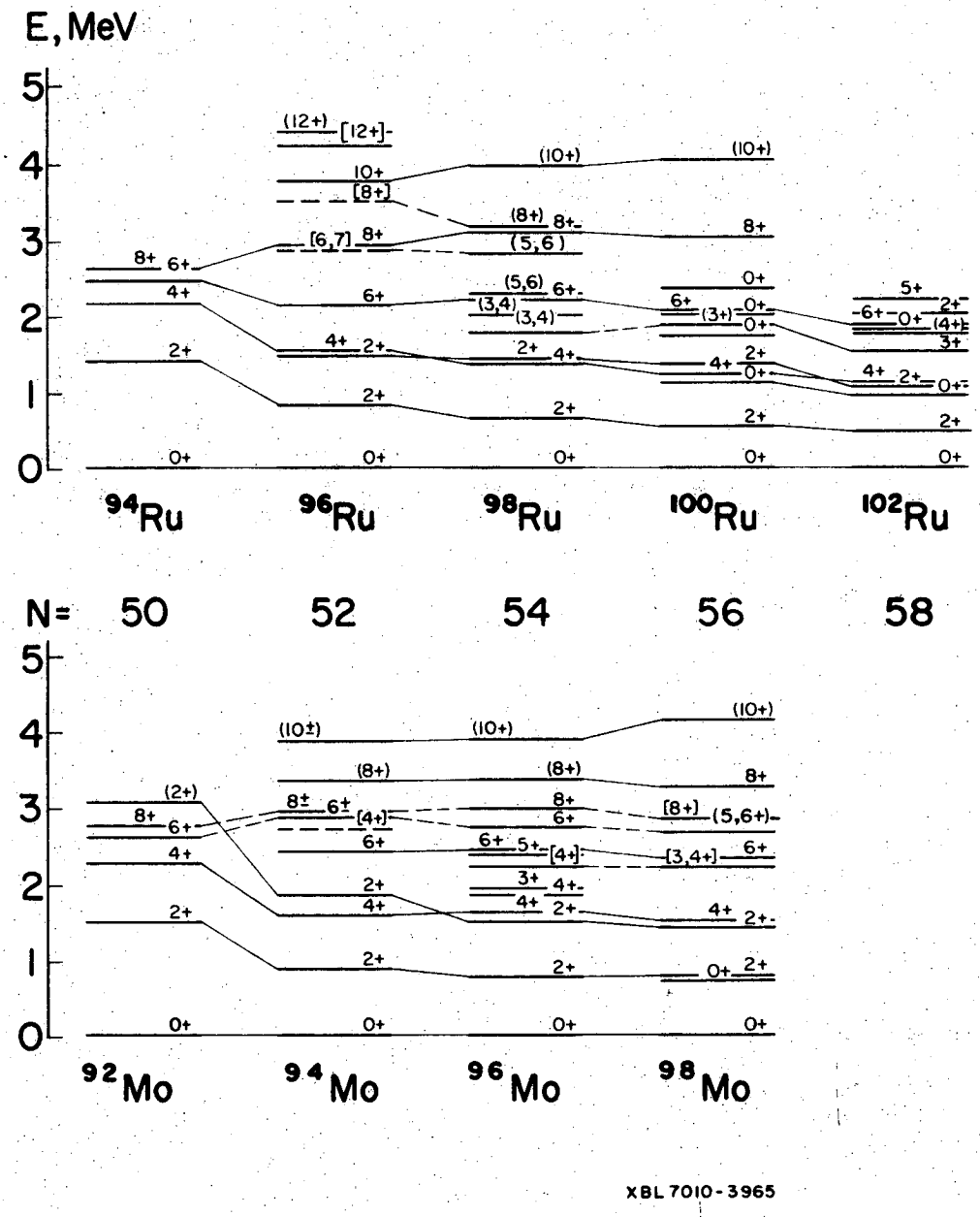
E, MeV
5
4
3
2
1
0
94Ru
96Ru
98Ru
100Ru
102Ru
N= 50 52 54 56 58
92Mo
94Mo
96Mo
98Mo
XBL 7010-3965

Fig. 12

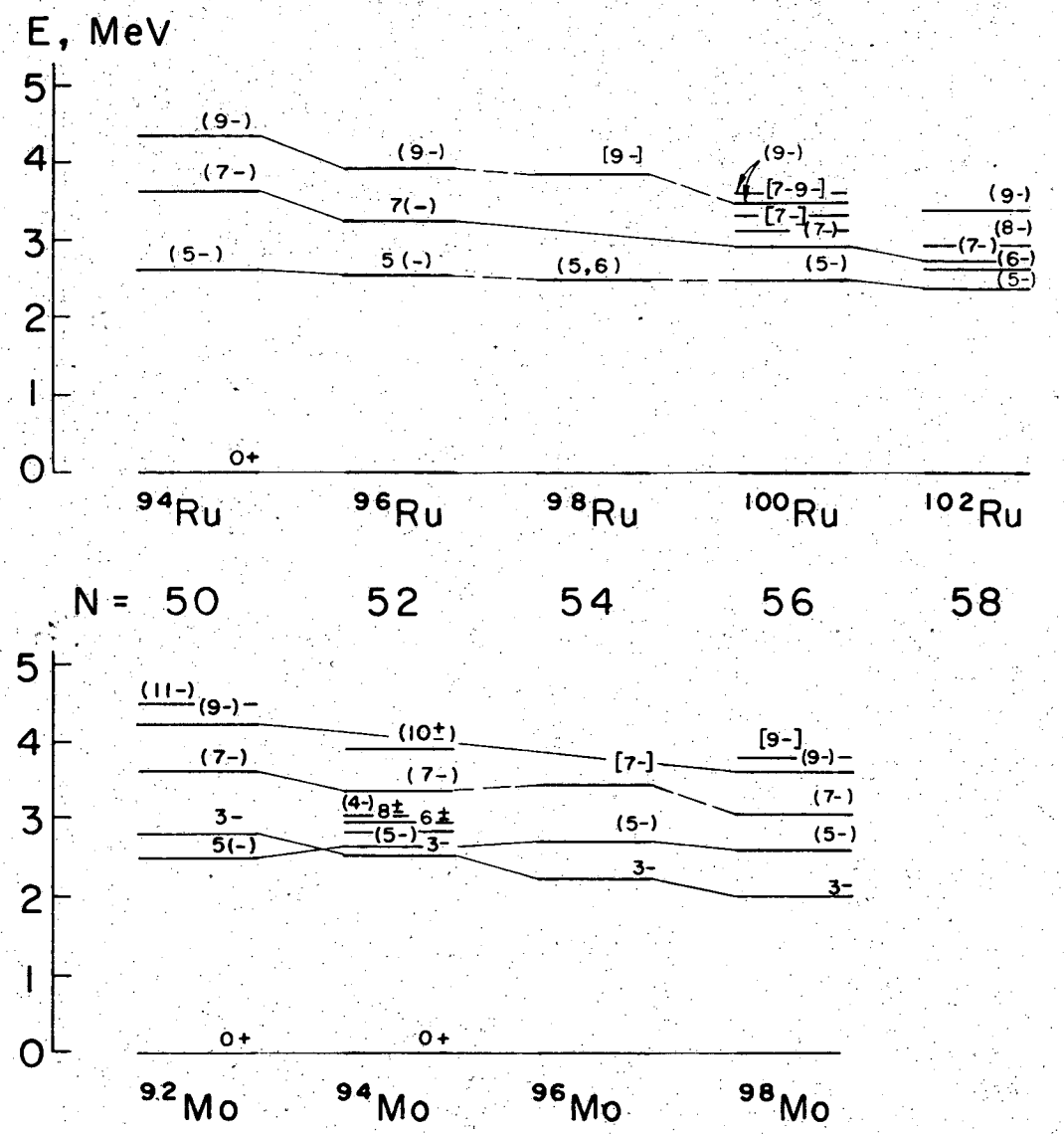
E, MeV
5
4
3
2
1
0
(9-)
(7-)
(5-)
0+
(9-)
7(-)
5(-)
[9-]
(5,6)
(9-)
[7-9-]
[7-]
(7-)
(5-)
(9-)
(8-)
(7-)
(6-)
(5-)
94Ru
96Ru
98Ru
100Ru
102Ru
N = 50
52
54
56
58
(11-)
(9-)
(7-)
3-
5(-)
(10±)
(7-)
(4-)
8±
6±
(5-)
3-
0+
0+
[7-]
(5-)
3-
[9-]
(9-)
(7-)
(5-)
3-
92Mo
94Mo
96Mo
98Mo
XBL7010-3964

Fig. 13

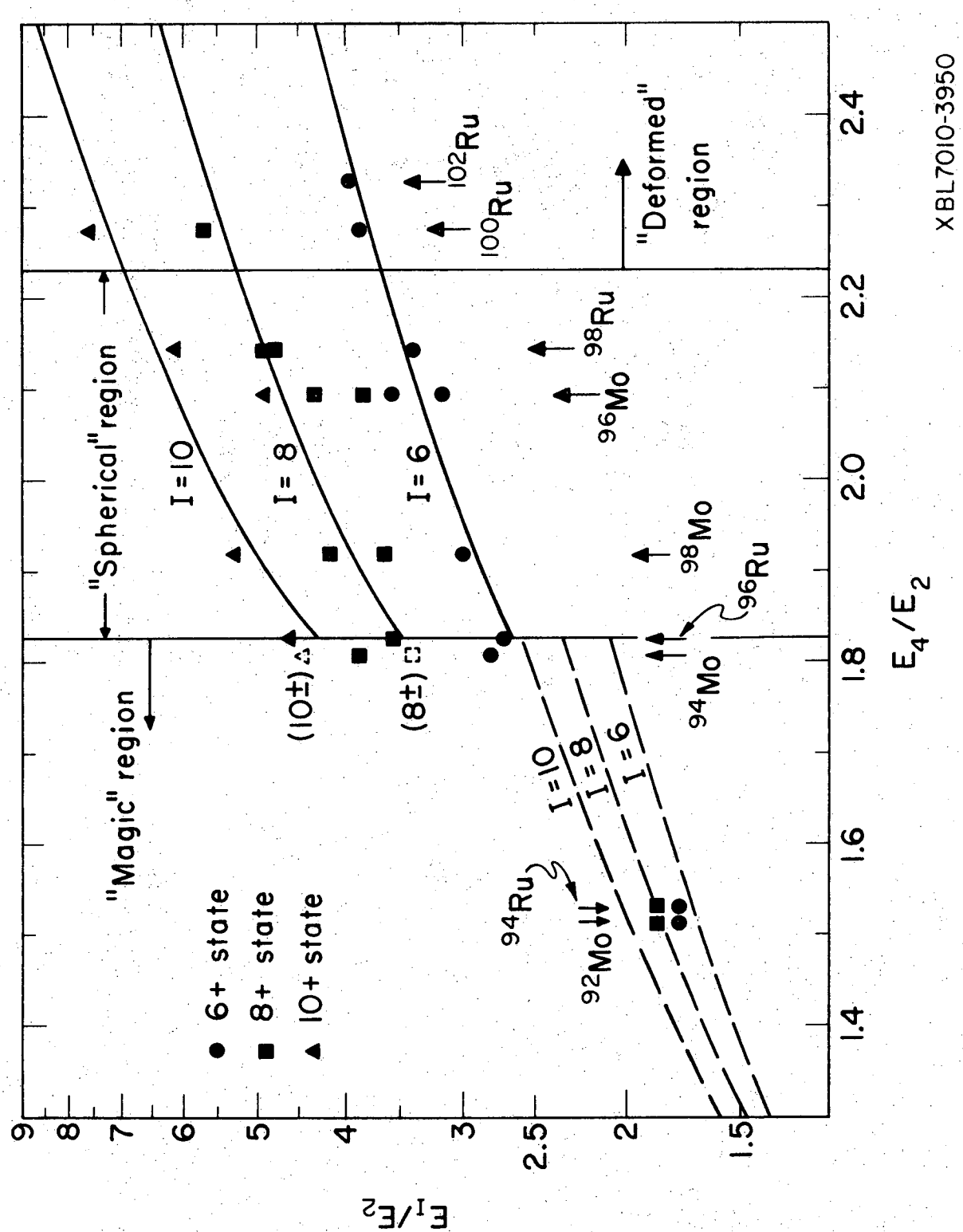
"Spherical" region
"Magic" region
"Deformed" region
I=10
I=8
I=6
(10±)
(8±)
6+ state
8+ state
10+ state
^{102}Ru
^{100}Ru
^{98}Ru
^{96}Mo
^{98}Mo
^{96}Ru
^{94}Mo
^{94}Ru
^{92}Mo
E_4/E_2
E_I/E_2
XBL7010-3950

Fig. 14

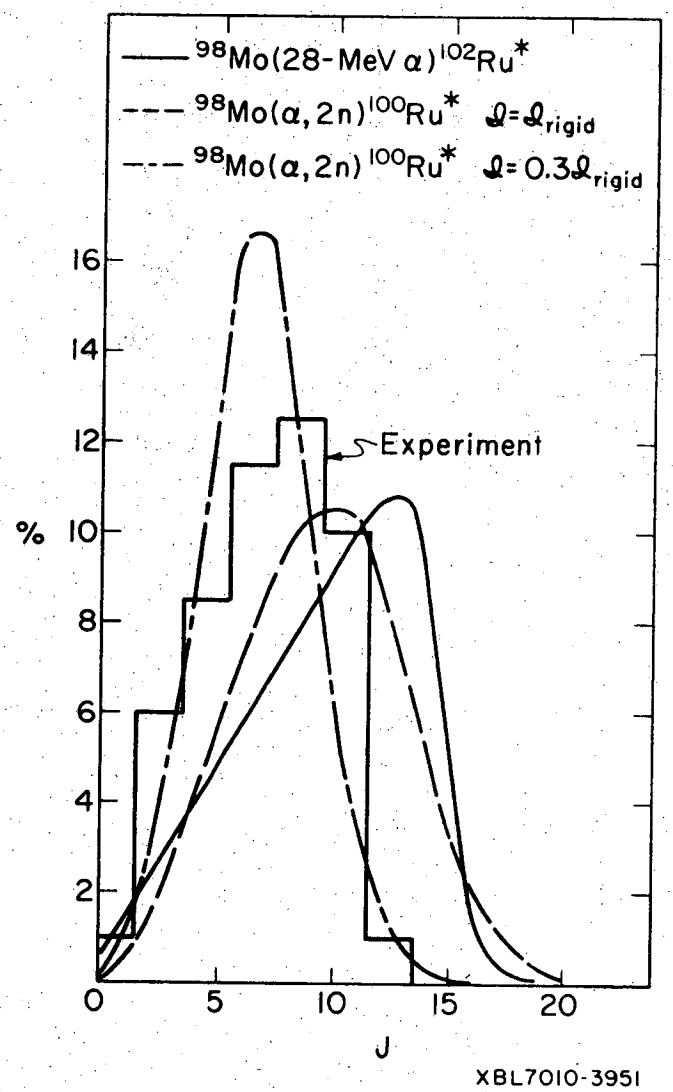
^{98}Mo(28-MeV α)^{102}Ru*
^{98}Mo(α, 2n)^{100}Ru* $\mathcal{J}=\mathcal{J}_{rigid}$
^{98}Mo(α, 2n)^{100}Ru* $\mathcal{J}=0.3\mathcal{J}_{rigid}$
Experiment
%
16
14
12
10
8
6
4
2
0
5
10
15
20
J
XBL7010-3951

Fig. 15

LEGAL NOTICE

This report was prepared as an account of work sponsored by the United States Government. Neither the United States nor the United States Atomic Energy Commission, nor any of their employees, nor any of their contractors, subcontractors, or their employees, makes any warranty, express or implied, or assumes any legal liability or responsibility for the accuracy, completeness or usefulness of any information, apparatus, product or process disclosed, or represents that its use would not infringe privately owned rights.

TECHNICAL INFORMATION DIVISION
LAWRENCE RADIATION LABORATORY
UNIVERSITY OF CALIFORNIA
BERKELEY, CALIFORNIA 94720